

Table 5. Proliferative Uterine Endometrial Lesions in Rats Given Low-doses of BPA*

Dose	Incidence of lesions (%)			
	Hyperplasia			Adenocarcinoma**
	+	++	+++	
0 mg/kg/day	21	21	13	33
0.006 mg/kg/day	20	20	17	33
6 mg/kg/day	13	47	17	20

*: Yoshida *et al.*, J Reprod Dev 2004; 50: 349–360.

** : All adenocarcinomas in the three groups were well differentiated and limited to the uterus.

(80 ppm) detected in plastic plates⁸⁷. The treatment did not exert any influences on the reproductive system of female offspring in either treated group, in terms of prepubertal uterine growth and gland-genesis, vaginal opening and gonadotropin secretion. After maturation also, no effects were evident with regard to estrous cyclicity, age-matched sequential changes of the reproductive organs, and uterine carcinogenesis until 15 months of age (Table 5). The results demonstrated that maternal exposure to BPA at human exposure-levels did not have any adverse effects on the female reproductive organs of offspring in rats⁸⁸.

For determination of effects of EDCs on offspring by maternal treatment, biotransfer of the chemicals from dam to offspring is crucial, because the impact is fundamentally related to the serum EDC level⁴⁰. However, data for transfer of the test chemical via the placenta or milk to offspring, or toxicokinetics of low-dose EDCs are very limited⁸⁹. In one of our studies, NP at 10 and 100 mg/kg doses was transferred from dams to their offspring via the milk, but the compound could not be detected in their serum or liver⁷³. Furthermore, BPA levels in the milk of dams, and those in the serum and liver in offspring were comparable between control and treated groups, although the serum level of BPA in dams receiving 6 mg/kg was significantly elevated⁸⁸.

Quite recently, it was reported that cadmium has potent estrogen-like activity *in vivo*⁹⁰. Thus, exposure to low-dose cadmium (a single ip injection at a dose of 5 µg/kg) increased uterine net weight accompanied by proliferation of the endometrium, promoted growth and development of the mammary glands, and induced hormone-regulated genes in ovariectomized rats. In utero exposure to the metal (i.p. injections of 0.5 or 5 µg/kg on days 12 and 17 gestation) mimicked also the effects of estrogens, and female offspring experienced an earlier onset of puberty and an increase in the epithelial area and the number of terminal end buds in the mammary gland. The amounts of cadmium used in the study were environmentally relevant, because the WHO-recommended Provisional Tolerable Weekly Intake Level is 7 µg/kg/week. Although the administration route was intraperitoneal, not oral, the ability of environmentally relevant amounts of cadmium to mimic the effects of estradiol is very important and the metal may represent a new class of EDC.

Species Differences in Toxicologic/carcinogenic Effects of EDCs, Effects of EDCs based on the Molecular Biology and Extrapolation of the Effects to Humans

It is well known that the toxicokinetics of chemicals in animals are influenced by many factors, including species, strain, sex, age, dosage and/or administration method, as mentioned above. In particular, species differences are very important for the risk assessment in humans. Species differences in occurrence of toxicologic/carcinogenic effects of EDCs may be an indication of variation in endogenous hormonal factors, in addition to susceptibility to exogenous agents. Mice are generally more sensitive to estrogens than rats, and uterine adenocarcinomas can be induced in mice by estrogen alone, but not in rats. In mice, perinatal exposure to estrogens was found to induce ovary-independent proliferation of the vaginal epithelium, which could not be abolished by ovariectomy⁹¹. On the other hand, the vagina in rats neonatally exposed to high-dose t-OP became atrophic immediately after ovariectomy³⁴. Adenocarcinoma development in the ENNG-initiated endometrium of Donryu rats exposed to high-dose t-OP was also ovary-dependent⁶⁴. In mice, however, E2 promoted uterine adenocarcinoma development ovary-independently⁵⁶. Differences in the reaction to estrogens or EDCs with estrogenic activity may help to explain species differences in toxicity/carcinogenicity, though further studies on this point, focusing on metabolism of estrogens or EDCs and localization of ER expression, are needed.

The prenatal and/or neonatal periods are more sensitive to estrogens, and also EDCs, than the adult period. As mentioned above, it has been pointed out that tamoxifen increases the risk of endometrial cancer in women. In rodents, TAM can induce uterine carcinomas when given to newborn animals, but not adults. Similarly, 2-OHE2 has weak estrogenic, but not carcinogenic effects, although 4-OHE2 is a potent estrogenic catechol causing uterine tumors in adult mice. However, both catechols induced tumors when given on days 1–5 of neonatal life, although carcinogenic activity of 4-OHE2 is stronger than that of 2-OHE2⁹². Further studies on age-dependent differences in the mechanism of EDCs' effects on the female genital organs are also needed.

Various methods such as DNA micro-array techniques based on gene expression levels have recently been used for the evaluation of hazardous effects of various chemicals, because they should reveal very early changes. Up till now, however, there have only been a few reports concerning EDCs. The fact that changes in ontogenic expression of ER alpha and not of ER beta occur in the fetal female rat reproductive tract, provides fundamental information critical for clarifying species-specific physiological roles of ER subtypes during fetal development and for investigating the tissue-specific mechanisms underlying prenatal responses to estrogen and E2 agonists⁹³. Genome-wide analysis of early gene expression has furthermore suggested a basis for the

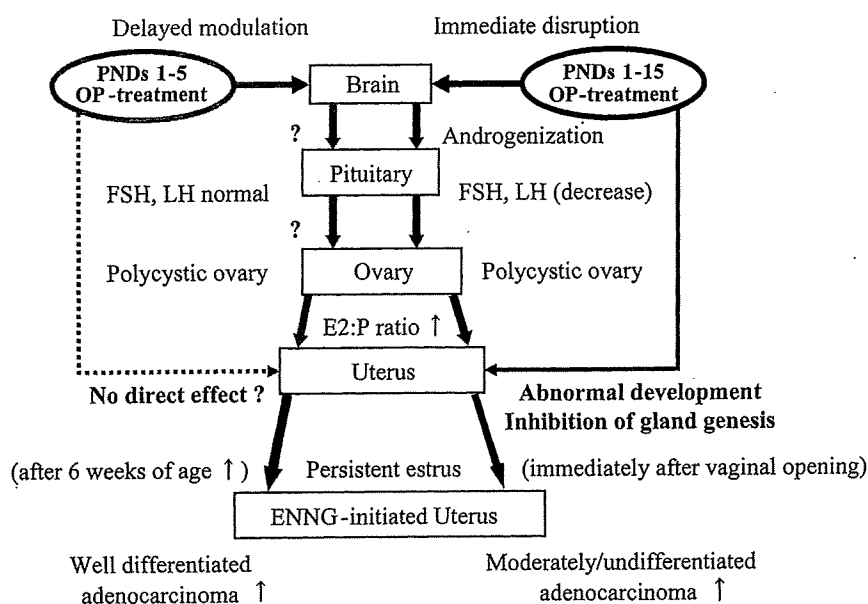


Fig. 3. Hypothesis of the scheme for "androgenization effects" or "delayed modulation effects" on the hypothalamo-pituitary-gonadal system in rats exposed neonatally to high-dose OP.

drastic uterotrophic effects following estrogen administration⁹⁴. Although DNA micro-array techniques presently demonstrate problems with reliability and reproducibility, future precise analysis should facilitate understanding of the mechanisms underlying effects of estrogenic EDCs⁹⁵.

Almost all EDCs exist at only very low concentrations in the environment, but humans may be exposed for long periods. In many animal studies, various toxicologic effects of EDCs on the female genital organs were demonstrated when very high doses were given, but no obvious effects were detected with low-doses. In humans also, low doses may show no adverse effects, because of homeostasis, although there are notable exceptions in animal and human studies. In fish, the ova-testis is known to be a good indicator of estrogenic effects of EDCs in females, but in female rodents, we are still lacking a consensus regarding equivalent reliable endpoint markers. Thus, more comprehensive studies of the endocrinological, morphological and also biomolecular aspects are necessary in animal studies using rodents for extrapolation of EDCs' effects to humans.

Conclusion

It is well known that the prenatal and/or neonatal period is particularly sensitive to various chemicals, including EDCs, in humans and rodents. Inappropriate exposure may exert irreversible influence, resulting in androgenization of the female genital system. In addition, it has also been reported that a delayed influence may be exerted. Neonatal exposure to a high dose of t-OP (100 mg/kg s.c. injection

every other day from PND 1 to PND 15) induced various long-term persistent irreversible effects on the female reproductive system of Donryu rats, such as lower gonadotropin levels at prepuberty, inhibition of uterine gland genesis, persistent estrus shown by vaginal cytology and polycystic ovaries. Neonatal treatment of high-dose EDCs having estrogenic activity can thus affect gonadotropin secretion during the developmental period of sexual maturation with direct masculinization of the hypothalamic function. Abnormal differentiation in the developing rat uteri may be induced via abnormal ER expression and subsequent alteration of cell proliferating activity. However, exposure limited to the first 5 days after birth to 100 mg/kg t-OP caused "delayed" influence which was characterized by accelerated appearance of atrophic ovary, manifested by an early-occurring and long-term continuing persistent estrus status after puberty, whereas no abnormalities could be found with regard to growth and development of the reproductive organs and the hypothalamo-pituitary-gonadal control system up to maturation. The hypothetical scheme for "androgenization effects" or "delayed modulation effects" on the hypothalamo-pituitary-gonadal system in rats exposed neonatally to high-dose OP is shown in Fig. 3.

On the other hand, the most notable effect on the female reproductive system when normal cycling rats were exposed to a high-dose of t-OP for a short time (28 days), was disappearance of the estrous cycle, and no clear changes were detected in other parameters such as uterine weight and morphology. These results indicate that the vaginal smear is the most sensitive parameter for the detection of effects of EDCs in normal cycling rats.

Well or moderately differentiated adenocarcinomas

were increased in Donryu rats initiated by ENNG, when high dose t-OP was given subcutaneously during adulthood. Neonatal exposure to a high dose of t-OP also showed promoting effects on uterine adenocarcinoma development in a two-stage rat uterine carcinogenesis model using Donryu rats, with slight to higher malignancy with more prolonged treatment.

For the risk assessment of EDCs to human health, it is very important to investigate the effects of low doses at actual human exposure levels, because the concentrations of agents, including alkylphenols and BPA, in the environment are very low. In addition, the main exposure route to EDCs is oral, not subcutaneous, in humans. Thus, we have focused on effects of maternal exposure to low doses of EDCs, such as NP and BPA, by the oral route, which have shown no effects on growth and development of the female reproductive system or uterine carcinogenesis. Transfer of low doses of BPA from dams to offspring via the placenta and/or milk was not unequivocal, although NP was transferred when relatively high doses were given.

These results indicate that dietary exposure to low doses of EDCs might not induce any adverse effects on the female genital system in mammals, including humans, because of the effects of homeostasis and clearance from the blood stream on first passage through the liver.

References

1. Maekawa A, Takahashi M, Ando J, and Yoshida M. Uterine carcinogenesis by chemicals/hormones in rodents. *J Toxicol Pathol* 1999; **12**: 1–11.
2. Zeil HK. Estrogen's role in endometrial cancer. *Obstet Gynecol* 1982; **60**: 509–515.
3. Fox H. Endometrial carcinogenesis and its relation to estrogens. *Pathol Res Pract* 1984; **179**: 13–19.
4. Nagaoka T, Takegawa K, Takeuchi M, and Maekawa A. Effects of reproduction on spontaneous development of endometrial adenocarcinomas and mammary tumors in Donryu rats. *Jpn J Cancer Res* 2000; **91**: 375–382.
5. Ando-Lu J, Takahashi M, Imai S, Ishihara R, Kitamura T, Iijima T, Takano S, Nishiyama K, Suzuki K, and Maekawa A. High-yield induction of uterine endometrial adenocarcinomas in Donryu rats by a single intra-uterine administration of N-ethyl-N'-nitro-N-nitrosoguanidine via the vagina. *Jpn J Cancer Res* 1994; **85**: 789–793.
6. Vollmer G. Endometrial cancer: experimental models useful for studies on molecular aspects of endometrial cancer and carcinogenesis. *Endocrine-Related Cancer* 2003; **10**: 23–42.
7. Hoare RM. Comparative developmental aspects of selected organ system. II. Gastrointestinal and urogenital systems. *Environ Health Perspect* 1976; **18**: 61–66.
8. Branham WS, Sheehan DM, Zehr DR, Ridlon E, and Nelson CJ. The postnatal ontogeny of rat uterine glands and age-related effects of 17 β -estradiol. *Endocrinology* 1985; **117**: 2229–2237.
9. Fishman RB, Branham WS, Streck RD, and Sheehan DM. Ontogeny of estrogen receptor messenger ribonucleic acid expression in the postnatal rat uterus. *Biol Reprod* 1996; **55**: 1221–1230.
10. Cheng HC and Johnson DC. Serum estrogens and gonadotropins in developing androgenized and normal female rats. *Neuroendocrinology* 1974; **13**: 357–365.
11. Dussault JH, Walker P, Dubois JD, and Labrie F. The development of the hypothalamo-pituitary axis in the neonatal rat: Sexual maturation in male and female rats assessed by hypothalamic LHRH and pituitary and serum LH and FSH concentrations. *Can J Physiol Pharmacol* 1977; **55**: 1091–1097.
12. Sell S, Nichols M, Becker FF, and Leffert HL. Hepatocyte proliferation and α 1-fetoprotein in pregnant, neonatal, and partially hepatectomized rats. *Cancer Res* 1974; **34**: 865–871.
13. Meijs-Roelofs HM and Kramer P. Maturation of the inhibitory feedback action of oestrogen on follicle-stimulating hormone secretion in the immature female rat: A role for alpha-fetoprotein. *J Endocrinol* 1979; **81**: 199–208.
14. Gorski RA, Gordon JH, Shryne JE, and Southam AM. Evidence for a morphological sex difference within the medial preoptic area of rat brain. *Brain Res* 1978; **148**: 333–346.
15. Jacobson CD, Csernus VJ, Shryne JE, and Gorski RA. The influence of gonadectomy, androgen exposure or a gonadal graft in the neonatal rat on the volume of the sexually dimorphic nucleus of the preoptic area. *J Neurosci* 1981; **1**: 1142–1147.
16. Doehler KD. The pre- and postnatal influence of hormones and neurotransmitters on sexual differentiation of the mammalian hypothalamus. *Int Rev Cytology* 1991; **131**: 1–57.
17. Houtsmuller EJ, Brand T, de Jonge FH, Joosten RN, Van de Poll NE, and Slob AK. SDN-POA volume, sexual behavior and preference of male rats affected by perinatal treatment with ATD. *Physiol Behav* 1994; **56**: 535–541.
18. Davis EC, Popper P, and Gorski RA. The role of apoptosis in sexual differentiation of the rat sexually dimorphic nucleus of the preoptic area. *Brain Res* 1996; **734**: 10–18.
19. Furguson SA, Scallet AC, Flynn KM, Meredith JM, and Schwetz BA. Developmental neurotoxicity of endocrine disruptors: focus on estrogen. *Neurotoxicol* 2000; **21**: 947–956.
20. Doehler KD and Jarzab B. The influence of hormone antagonists on sexual differentiation of the brain. *J Clean Technol Environ Toxicol & Occup Med* 1998; **7**: 195–220.
21. Pinos H, Collado P, Rodrigues-Zafra M, Rodriguez C, Segovia S, and Guillamon A. The development of sex difference in the locus coeruleus of the rats. *Brain Res Bull* 2001; **56**: 73–78.
22. Orikasa C, Kondo Y, Hayashi S, McEwen BS, and Sakuma Y. Sexually dimorphic expression of estrogen receptor β in the anteroventral periventricular nucleus of the rat preoptic area: Implication in luteinizing hormone surge. *Proc Natl Acad Sci USA* 2002; **99**: 3306–3311.
23. Henry WW Jr, Medlock KL, Sheehan DM, and Scallet AC. Detection of estrogen receptor (ER) in the hypothalamus using rat anti-ER monoclonal IgG with the unlabeled antibody method. *Histochem* 1991; **96**: 157–162.
24. Kuiper GGJM, Carlsson B, Grandien K, Enmark E, Haggblad J, Nilsson S, and Gustafsson JA. Comparison of the ligand binding specificity and transcript tissue distribution of estrogen receptors α and β . *Endocrinol* 1997; **138**: 863–870.

25. Del Vecchio FR. Normal development, growth, and aging of the female genital tract. In: Pathology of the Aging Rat (Vol. 1), Mohr U, Dungworth DL and Capen CC (eds), Washington DC: ILSI Press, 331–336, 1992.
26. Katsuda S, Yoshida M, Watanabe T, Kuroda H, Ando-Lu J, Takahashi M, Hayashi H, and Maekawa A. Estrogen receptor mRNA in uteri of normal estrous cycling and ovariectomized rats by in situ hybridization. *Proc Soc Exp Biol Med* 1999; **221**: 207–214.
27. Ando-Lu J, Sasahara K, Nishiyama K, Takano S, Takahashi M, Yoshida M, and Maekawa A. Strain-differences in proliferative activity of uterine endometrial cells in Donryu and Fischer 344 rats. *Exp Toxic Pathol* 1998; **50**: 185–190.
28. Nagaoka T, Takeuchi M, Onodera H, Matsushima Y, Ando-Lu J, and Maekawa A. Sequential observation of spontaneous endometrial adenocarcinoma development in Donryu rats. *Toxicol Pathol* 1994; **22**: 261–269.
29. OECD. OECD guideline and protocol for the prevalidation of the rat uterotrophic screening assay. ENV/JM/TG/EDTA(99)2/ANN1. Joint Meeting of the Chemical Committee and the Working Party on Chemicals, Paris, 1999.
30. Dodge JA, Glasebrook AL, Magee DE, Phillips DL, Sato M, Short LL, and Bryant HU. Environmental estrogens: effects on cholesterol lowering and bone in the ovariectomized rat. *J Steroid Biochem Mol Biol* 1996; **59**: 155–161.
31. Iguchi T and Takasugi N. Occurrence of permanent changes in vaginal and uterine epithelia in mice treated neonatally with progestin, estrogen, and aromatizable or non-aromatizable androgens. *Endocrinol Jpn* 1976; **23**: 327–332.
32. Colborn T and Clement C. Chemically-induced alterations in sexual and functional development: the wildlife/human connection. In: *Advances in Modern Environmental Toxicology*. Colborn T and Clement C (eds), Princeton, NJ: Princeton Scientific Publishing, 1–403, 1992.
33. Blake CA and Ashiru OA. Disruption of rat estrous cyclicity by the environmental estrogen 4-tert-octylphenol. *Proc Soc Exp Biol Med* 1997; **216**: 446–451.
34. Katsuda S, Yoshida M, Watanabe G, Taya K, and Maekawa A. Irreversible effects of neonatal exposure to p-tert-octylphenol on the reproductive tract in female rats. *Toxicol Appl Pharmacol* 2000; **165**: 217–226.
35. Yoshida M, Takenaka A, Katsuda S, Kurokawa Y, and Maekawa A. Neonatal exposure to p-tert-octylphenol causes abnormal expression of estrogen receptor α and subsequent alteration of cell proliferating activity in the developing Donryu rat uterus. *Toxicol Pathol* 2002; **30**: 357–364.
36. MacLusky NJ and Naftolin F. Sexual differentiation of the central nervous system. *Science* 1981; **211**: 1294–1303.
37. Yoshida M, Katsuda S, Tanimoto T, Asai S, Nakae D, Kurokawa Y, Taya K, and Maekawa A. Induction of different types of uterine adenocarcinomas in Donryu rats due to neonatal exposure to high-dose p-t-octylphenol for different periods. *Carcinogenesis* 2002; **23**: 1745–1750.
38. Blake CA and Boockfor FR. Chronic administration of the environmental pollutant 4-tert-octylphenol to adult male rats interferes with the secretion of luteinizing hormone, follicle-stimulating hormone, prolactin, and testosterone. *Biol Reprod* 1997; **57**: 255–266.
39. Boockfor FR and Blake CA. Chronic administration of 4-tert-octylphenol to adult male rats causes shrinkage of the testes and male accessory sex organs, disrupts spermatogenesis, and increases the incidence of sperm deformities. *Biol Reprod* 1997; **57**: 267–277.
40. Katsuda S, Yoshida M, Isagawa S, Asagawa Y, Kuroda H, Watanabe T, Ando J, Takahashi M, and Maekawa A. Dose- and treatment duration-related effects of p-tert-octylphenol on female rats. *Reprod Toxicol* 2000; **14**: 119–126.
41. Yoshida M, Katsuda S, Ando J, Kuroda H, Takahashi M, and Maekawa A. Subcutaneous treatment of p-tert-octylphenol exerts estrogenic activity on the female reproductive tract in normal cycling rats of two different strains. *Toxicol Lett* 2000; **116**: 89–101.
42. Nagaoka T, Takegawa K, and Maekawa A. The relationship between endocrine imbalance and alteration of rat vaginal epithelium. *J Toxicol Pathol* 2002; **15**: 103–109.
43. Aso S, Anai M, Noda S, Imatanaka N, Yamasaki K, and Maekawa A. Twenty-eight-day repeated-dose toxicity studies for detection of weak endocrine disrupting effects of nonylphenol and atrazine in female rats. *J Toxicol Pathol* 2000; **13**: 13–20.
44. Yamasaki K, Sawaki M, Noda S, Muroi T, and Maekawa A. Immature rat uterotrophic assay of diethylstilbestrol, ethynyl estradiol and atrazine. *J Toxicol Pathol* 2000; **13**: 145–149.
45. Herbst AL, Ulfelder H, and Poskanzer DC. Adenocarcinoma of the vagina. Association of maternal stilbestrol therapy with tumor appearance in young women. *N Engl J Med* 1971; **184**: 878–881.
46. Marselos M and Tomatis L. Diethylstilbestrol. II. Pharmacology, toxicology and carcinogenicity in experimental animals. *Eur J Cancer* 1993; **29**: 149–155.
47. Newbold RR and McLachlan JA. Vaginal adenosis and adenocarcinoma in mice exposed prenatally or neonatally to diethylstilbestrol. *Cancer Res* 1982; **42**: 2003–2011.
48. Walker BE. Uterine tumors in old female mice exposed prenatally to diethylstilbestrol. *J Natl Cancer Inst* 1983; **70**: 477–484.
49. Kitamura T, Nishimura S, Sasahara K, Yoshida M, Ando J, Takahashi M, Shirai T, and Maekawa A. Transplacental administration of diethylstilbestrol (DES) causes lesions in female reproductive organs of Donryu rats, including endometrial neoplasia. *Cancer Lett* 1999; **141**: 219–228.
50. Pasqualini JR, Sumida C, and Giambiagi N. Pharmacodynamic and biological effects of anti-estrogens in different models. *J Steroid Biochem* 1988; **31**: 613–643.
51. Killackey MA, Hakes TB, and Pierce VK. Endometrial adenocarcinoma in breast cancer patients receiving antiestrogens. *Cancer Treat Rep* 1985; **69**: 237–238.
52. IARC. Tamoxifen. In: *IARC Monographs on the Evaluation of Carcinogenic Risks to Humans* (Vol. 66), Lyon: IARC, 253–365, 1996.
53. Newbold RR, Jefferson WN, Padilla-Burgos E, and Bullock BC. Uterine carcinoma in mice treated neonatally with tamoxifen. *Carcinogenesis* 1997; **18**: 2293–2298.
54. Carthew P, Edwards RE, Nolan BM, Martin EA, Heydon RT, White INH, and Tucker MJ. Tamoxifen induces endometrial and vaginal cancer in rats in the absence of endometrial hyperplasia. *Carcinogenesis* 2000; **21**: 793–797.
55. Yoshida M, Kudoh K, Katsuda S, Takahashi M, Ando J, and Maekawa A. Inhibitory effects of uterine endometrial carcinogenesis in Donryu rats by tamoxifen. *Cancer Lett* 1998; **134**: 43–51.
56. Takahashi M, Shimomoto M, Miyajima K, Iizuka S, Watanabe T, Yoshida M, Kurokawa Y, and Maekawa A.

- Promotion, but not progression, effects of tamoxifen on uterine carcinogenesis in mice initiated with N-ethyl-N'-nitro-N-nitrosoguanidine. *Carcinogenesis* 2002; **23**: 1549-1555.
57. Pinter A, Torok G, Borzsonyi M, Surjan A, Csik M, Kelecsenyi Z, and Kocsis Z. Long-term carcinogenicity bioassay of the herbicide atrazine in F344 rats. *Neoplasia* 1990; **37**: 533-544.
 58. Watanabe T, Kashida Y, Ueda M, Onodera H, Hirose M, and Mitsumori K. Promoting effects of ethinylestradiol but not atrazine on N-ethyl-N-nitrosourea-induced uterine carcinogenesis in ICR mice. *J Toxicol Pathol* 2003; **16**: 139-145.
 59. IPCS (International Programme on Chemical Safety). Vinclozolin. In: *Pesticide Residues in Food-1995* (Joint FAO/WHO Meeting of Pesticide Residues), Geneva: WHO, 375-404, 1996.
 60. Rier SE, Martin DC, Bowman RE, Dmowski WP, and Becker JL. Endometriosis in rhesus monkeys (*Macaca mulatta*) following chronic exposure to 2,3,7,8-tetrachlorodibenzo-p-dioxin. *Fund Appl Toxicol* 1993; **21**: 433-441.
 61. Moriya M, Mitsumori K, Kato K, Miyazawa T, and Shirasu Y. Carcinogenicity of N-nitroso-ethylenethiourea in female mice. *Cancer Lett* 1979; **7**: 339-342.
 62. Yoshida A, Harada T, Hayashi S, Mori I, Miyajima H, and Maita K. Endometrial carcinogenesis induced by concurrent oral administration of ethylenethiourea and sodium nitrite in mice. *Carcinogenesis* 1994; **15**: 2311-2318.
 63. Nishiyama K, Ando-Lu J, Nishimura S, Takahashi M, Yoshida M, Sasahara K, Miyajima K, and Maekawa A. Initiating and promoting effects of concurrent oral administration of ethylenethiourea and sodium nitrite on uterine endometrial adenocarcinoma development in Donryu rats. In *Vivo* 1998; **12**: 363-368.
 64. Katsuda S, Yoshida M, Kuroda H, Ando J, Takahashi M, Kurokawa Y, Watanabe G, Taya K, and Maekawa A. Uterine adenocarcinoma in N-ethyl-N'-nitro-N-nitrosoguanidine-treated rats with high-dose exposure to p-tert-octylphenol during adulthood. *Jpn J Cancer Res* 2002; **93**: 117-124.
 65. Zhu BT and Conney AH. Functional role of estrogen metabolism in target cells: review and perspectives. *Carcinogenesis* 1998; **19**: 1-27.
 66. Takahashi M, Shimomoto T, Miyajima K, Yoshida M, Katashima S, Uematsu F, Maekawa A, and Nakae D. Effects of estrogens and metabolites on endometrial carcinogenesis in young adult mice initiated with N-ethyl-N'-nitro-N-nitrosoguanidine. *Cancer Lett* 2004; in press.
 67. Kojima T, Tanaka T, and Mori H. Chemoprevention of spontaneous endometrial cancer in female Donryu rats by dietary indole-3-carbinol. *Cancer Res* 1994; **54**: 1446-1449.
 68. Certa H, Fedtke N, Wiegand HJ, Muller AMF, and Bolt HM. Toxicokinetics of p-tert-octylphenol in male Wistar rats. *Arch Toxicol* 1996; **71**: 112-122.
 69. Upmeyer A, Degan GH, Schuhmacher US, Certa H, and Bolt HM. Toxicokinetics of p-tert-octylphenol in female DA/Han rats after single i.v. and oral application. *Arch Toxicol* 1999; **73**: 217-222.
 70. NTP. NTP final report on the reproductive toxicity of nonylphenol (CAS# 84852-15-3) administered by gavage to Sprague-Dawley rats. NTP Report # RACB 94021, 1997.
 71. Chapin RE, Delaney J, Wang Y, Lanning L, Davis B, Collins B, Minz N, and Wolfe G. The effects of 4-nonylphenol in rats: a multi-generation reproduction study. *Toxicol Sci* 1999; **52**: 80-91.
 72. Nagano T, Wada K, Marumo H, Yoshimura S, and Ono H. Reproductive effects of nonylphenol in rats after gavage administration: a two-generation study. *Reprod Toxicol* 2001; **15**: 293-315.
 73. Yoshida M, Shimomoto T, Katashima S, Shirai T, Nakae D, Watanabe G, Taya K, and Maekawa A. Effects of maternal exposure to nonylphenol on growth and development of the female reproductive system and uterine carcinogenesis in rats. *J Toxicol Pathol* 2003; **16**: 259-266.
 74. Ashby J and Tinwell H. Uterotropic activity of bisphenol A in the immature rat. *Environ Health Perspect* 1998; **106**: 719-720.
 75. Morrissey RE, Lamb JC. IV, Morris RW, Chapin RE, Gulati DK, and Heindel JJ. Results and evaluations of 48 continuous breeding reproduction studies conducted in mice. *Fund Appl Toxicol* 1989; **13**: 747-777.
 76. Morrissey RE, George JJ, Price CJ, Tyl RW, Marr MC, and Kimmel CA. The developmental toxicity of bisphenol A in rats and mice. *Fund Appl Toxicol* 1987; **8**: 1294-1302.
 77. Nagao R, Saito Y, Usumi K, Kuwagata M, and Imai K. Reproductive function in rats exposed neonatally to bisphenol A and estradiol benzoate. *Reprod Toxicol* 1999; **13**: 303-311.
 78. Kwon S, Stedman DB, Ilswick RC, Cattley RC, and Welsch F. Pubertal development and reproductive functions of Crl:CD BR Sprague-Dawley rats exposed to bisphenol A during prenatal and postnatal development. *Toxicol Sci* 2000; **55**: 399-406.
 79. Sharpe RM, Fisher J, Milar MR, Jobling S, and Sumpter JS. Gestational and/or neonatal exposure of rats to environmental estrogenic chemicals results in reduced testis size and daily sperm production in adulthood. *Environ Health Perspect* 1995; **103**: 1136-1143.
 80. vom Saal FS, Cooke PS, Buchanan DL, Palanza P, Thayer KA, Nagel SC, Parmigiani S, and Welshons WV. A physiologically based approach to the study of bisphenol A and other estrogenic chemicals on the size of reproductive organs, daily sperm-production, and behavior. *Toxicol Ind Health* 1998; **14**: 239-260.
 81. Fisher JS, Turner KJ, Brown D, and Sharpe RM. Effects of neonatal exposure to estrogenic compounds on development of the excurrent ducts of the rat testis through puberty to adulthood. *Environ Health Perspect* 1999; **107**: 397-405.
 82. Howdeshell KL, Hotchkiss AK, Thayer KA, Vanderbergh JG, and vom Saal FS. Exposure to bisphenol A advances puberty. *Nature* 1999; **401**: 763-764.
 83. Ashby J, Tinwell H, and Haseman J. Lack of effects for low dose levels of bisphenol A and diethylstilbestrol on the prostate gland of CF1 mice exposed in utero. *Regul Toxicol Pharmacol* 1999; **30**: 156-166.
 84. Cagen SZ, Waechter JM Jr, Dimond SS, Breslin WJ, Butala JH, Jekat FW, Joiner RL, Shiotsuka RN, Veenstra GE, and Harris LR. Normal reproductive organ development in CF-1 mice following prenatal exposure to bisphenol A. *Toxicol Sci* 1999; **50**: 36-44.
 85. Cagen SZ, Waechter JM Jr, Dimond SS, Breslin WJ, Butala JH, Jekat FW, Joiner RL, Shiotsuka RN, Veenstra GE, and Harris LR. Normal reproductive organ development in

- Wistar rats exposed to bisphenol A in the drinking water. *Regul Toxicol Pharmacol* 1999; **30**: 130–139.
86. Tyl RW, Myers CB, Marr MC, Thomas BF, Keimowitz AR, Brine DR, Veselica MM, Fail PA, Chang TY, Seely JC, Joiner RL, Butala JH, Dimond SS, Cagen SZ, Shiotsuka RN, Stropp GD, and Waechter JM. Three-generation reproductive toxicity study of dietary bisphenol A in CD Sprague-Dawley rats. *Toxicol Sci* 2002; **68**: 121–146.
 87. Kawamura Y, Inoue K, Nakazawa H, Yamada T, and Maitani T. Cause of bisphenol A migration from cans for drinks and assessment of improved cans. *Syokuhin Eiseigaku Zasshi* 2001; **42**: 13–17.
 88. Yoshida M, Shimomoto T, Katashima S, Watanabe G, Taya K, and Maekawa A. Maternal exposure to low doses of bisphenol A has no effects on development of female reproductive tract and uterine carcinogenesis in Donryu rats. *J Reprod Dev* 2004; **50**: 349–360.
 89. Takahashi O and Oishi S. Disposition of orally administered 2,2-bis(4-hydroxyphenyl)propane (bisphenol A) in pregnant rats and the placental transfer to fetuses. *Environ Health Perspect* 2000; **108**: 931–935.
 90. Johnson MD, Kenney N, Stoica A, Hilakivi-Clarke L, Singh B, Chepko G, Clarke R, Sholler P, Lirio AA, Foss C, Reiter R, Trock B, Paik S, and Martin MB. Cadmium mimics the in vivo effects of estrogen in the uterus and mammary gland. *Nature Med* 2003; **9**: 1081–1084.
 91. Takasugi N. Cytological basis for permanent vaginal changes in mice treated neonatally with steroid hormones. *Int Rev Cytol* 1976; **44**: 193–224.
 92. Newbold RR and Liehr JG. Induction of uterine adenocarcinoma in CD-1 mice by catechol estrogens. *Cancer Res* 2000; **60**: 235–237.
 93. Okada A, Ohta Y, Buchanan DL, Sato T, Inoue S, Hiroi H, Muramatsu M, and Iguchi T. Changes in ontogenic expression of estrogen receptor α and not of estrogen receptor beta in the female rat reproductive tract. *J Molecular Endocrinol* 2002; **28**: 87–97.
 94. Watanabe H, Suzuki A, Mizutani T, Khono S, Lubahn DB, Handa H, and Iguchi T. Genome-wide analysis of changes in early gene expression induced by estrogen. *Genes to Cells* 2002; **7**: 497–507.
 95. Watanabe H and Iguchi T. Evaluation of endocrine disruptors based on gene expression using a DNA microarray. *Environ Sci* 2003; **10**: 061–067.

Regulation of naive T cell function by the NF- κ B2 pathway

Naozumi Ishimaru^{1,2}, Hidehiro Kishimoto³, Yoshio Hayashi² & Jonathan Sprent^{1,4}

T cell activation involves the orchestration of several signaling pathways, including that of the 'classical' transcription factor NF- κ B components NF- κ B1–RelA. The function of the 'nonclassical' NF- κ B2–RelB pathway is less clear, although T cells lacking components of this pathway have activation defects. Here we show that mice deficient in NF- κ B-inducing kinase have a complex phenotype consisting of immunosuppression mediated by CD25⁺Foxp3⁺ memory CD4⁺ cells and, in the absence of those cells, hyper-responsive naive CD4⁺ T cells, which caused autoimmune lesions after adoptive transfer into hosts deficient in recombination-activating genes. Biochemical studies indicated involvement of a cell-intrinsic mechanism in which NF- κ B2 (p100) limits nuclear translocation of NF- κ B1–RelA and thereby functions as a regulatory 'brake' for the activation of naive T cells.

The transcription factor NF- κ B is key in the regulation of many inflammatory processes of immune cells¹. The NF- κ B family consists of five subunits: NF- κ B1 (p105–p50), NF- κ B2 (p100–p52), RelA (p65), RelB and c-Rel. Hetero- or homodimers of these subunits can be translocated into the nucleus to bind to κ B sequences of neighboring 'target' genes, thus regulating the transcription of genes required for cell activation, survival and development². Two pathways of NF- κ B have been defined in immune cells³: the 'classical' pathway, which is initiated by complexes of NF- κ B1 and RelA, and an alternative or 'nonclassical' pathway, which is initiated by complexes of NF- κ B2 and RelB.

For T cells, stimulation via the T cell receptor (TCR) and costimulatory molecules such as CD28 leads to NF- κ B activation through a variety of intracellular signaling molecules⁴. Initially, TCR-CD28 signaling via many adaptor molecules leads to activation of protein kinase C- θ (PKC- θ)⁵. Thereafter, CARMA1–Bcl-10–MALT1 proteins 'downstream' of PKC- θ activate I κ B kinase (IKK) complexes, including IKK α , IKK β and the adaptor protein IKK γ (also called NEMO)^{6,7}. Activated IKK complexes then phosphorylate I κ B, releasing it from its constitutively bound state with cytoplasmic NF- κ B complexes (mainly NF- κ B1–RelA) that normally prevents NF- κ B complexes from translocating to the nucleus. Ubiquitination and degradation of I κ B by IKK complexes allows components of the classical NF- κ B pathway, especially p50–RelA, to be transported into the nucleus, thus promoting transcription of essential target genes required for survival, cytokine and chemokine production, upregulation of adhesion molecules, organogenesis and apoptosis in the immune system⁸. The classical NF- κ B pathway is especially important for the synthesis of interleukin 2 (IL-2) as well as IL-2 receptor (IL-2R, also called CD25) in T cells^{9,10}.

As for the alternative, nonclassical NF- κ B pathway, signals from specific cytokine receptors (such as the lymphotoxin- β receptor) activate NF- κ B-inducing kinase (NIK) as well as PKC- θ and CARMA1–Bcl-10–MALT1, which in turn activate homodimers of IKK α that are required for the cleavage of p100 to p52 (refs. 11–13). Complexes of p52 and RelB then translocate into the nucleus to regulate transcription of a different set of genes.

Studies of gene-knockout mice have demonstrated that individual members of the NF- κ B family have distinct roles *in vivo* in T cell function. Thus, T cell proliferation and T helper type 2 cytokine production is reduced in NF- κ B1-deficient (*Nfkb1*^{-/-}) mice, and these mice show increased susceptibility to experimental autoimmune encephalomyelitis, typhlocolitis and infection with *Leishmania major* but are resistant to asthma^{14–17}. RelA-deficient (*Rela*^{-/-}) mice have a phenotype that is embryonically lethal, but studies with fetal liver chimeras indicate that *Rela*^{-/-} T cells are functionally defective^{18,19}. RelB-deficient (*Relb*^{-/-}) mice are viable but develop systemic inflammation and severe anemia around 2–3 months of age, and the T cell and B cell functions of these mice are suppressed²⁰. NF- κ B2-deficient (*Nfkb2*^{-/-}) mice have B cell defects as well as T cell hyperplasia and hyperactivation of dendritic cells^{21,22}. Finally, mice deficient in c-Rel (*Rel*^{-/-}) have B cell defects, impaired T cell proliferative responses and reduced susceptibility to experimental autoimmune encephalomyelitis^{23,24}. Nevertheless, precise information about the functions of the individual NF- κ B family members on T cell function is still unclear.

The importance of NIK for NF- κ B activation has been demonstrated in studies of NIK-deficient (*Map3k14*^{-/-}) mice and also mice with lymphoplasia (*Map3k14*^{aly/aly} or 'aly/aly' mice), which carry a mutation of *Map3k14*. Functionally, NIK is key in regulating the

¹The Scripps Research Institute, La Jolla, California 92037, USA. ²Department of Oral Molecular Pathology, Institute of Health Biosciences, Tokushima University Graduate School, Tokushima 770-8504, Japan. ³Research Institute for Biological Sciences, Tokyo University of Science, Noda-City, Chiba 278-0022, Japan. ⁴Garvan Institute of Medical Research, Darlinghurst NSW 2010, Australia. Correspondence should be addressed to J.S. (j.sprent@garvan.org.au).

Received 27 January; accepted 26 April; published online 28 May 2006; doi:10.1038/ni1351

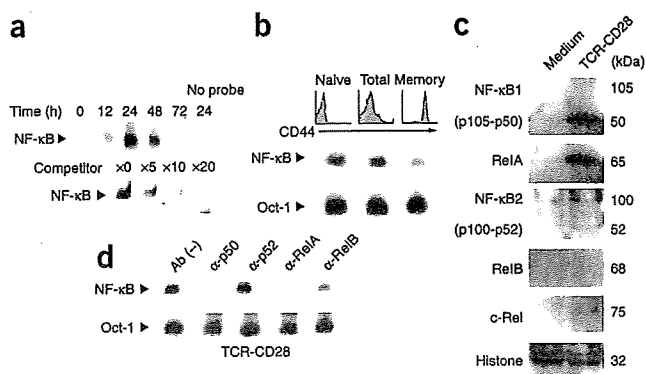


Figure 1 NF- κ B activation in CD4⁺ T cells. (a) EMSA of NF- κ B activity in nuclear extracts from CD4⁺ T cells from lymph nodes of B6 mice stimulated (times, above lanes) with crosslinked anti-TCR (1 μ g/ml) and anti-CD28 (20 μ g/ml). Below, EMSA with competitor (concentration, above lanes). (b) EMSA of NF- κ B and Oct-1 activity in nuclear extracts of total, naive CD44^{lo} or memory CD44^{hi} CD4⁺ T cells stimulated for 24 h by TCR-CD28 ligation as in a. Top, CD44 expression on the cells before culture, determined by flow cytometry. (c) Immunoblot for NF- κ B subunits in nuclear extracts of naive CD4⁺ T cells cultured in medium alone or activated for 24 h by TCR-CD28 ligation. (d) Antibody supershift assay of nuclear extracts from purified naive CD4⁺ T cells obtained from B6 lymph nodes; cells were stimulated for 24 h by TCR-CD28 ligation. Ab (-), no antibody; α -, antibody. Results are representative of three to five independent experiments.

processing of p100 to p52 through IKK α both in hematopoietic cells and osteoclasts^{25–27}. *Map3k14*^{-/-} and *aly/aly* mice lack lymph nodes, and, at least for *aly/aly* mice, T cells show defective proliferation and IL-2 production in response to stimulation with antibody to CD3 (anti-CD3)^{13,28,29}. In addition, NIK may be involved in the maintenance of central tolerance in the thymus³⁰. Moreover, *aly/aly* mice as well as *Relb*^{-/-} mice show signs of autoimmune disease^{20,31,32}. Despite those findings, the mechanism for the regulation of peripheral T cell activation through NIK has not been established.

Much of the data on the function of NIK has come from studies of T cell populations that have not been separated into individual subsets based on their activation status. Expression of certain surface markers, notably CD44, distinguishes mature T cells as those that are immunologically naive (naive T cells) versus those that have been primed through contact with environmental antigens (memory T cells)^{33,34}. In mice, low or intermediate expression of CD44 (CD44^{lo} or CD44^{int}) indicates a naive differentiation status, whereas CD44^{hi} cells have differentiated into memory cells. Here we examine the functions of NIK, both *in vivo* and *in vitro*, in purified subsets of naive and memory CD4⁺ cells.

RESULTS

NF- κ B1 in CD4⁺ cell activation

To define the kinetics of NF- κ B activation during the course of normal T cell activation, we analyzed the transcriptional activity of NF- κ B in stimulated CD4⁺ T cells from normal C57BL/6 (B6) mice by electrophoretic mobility-shift assay (EMSA) using an NF- κ B-binding DNA probe. After total CD4⁺ T cells were stimulated with plate-bound monoclonal antibodies (mAbs) to TCR and CD28, activation of NF- κ B, measured in nuclear extracts of the cells, reached a peak after 24 h and then decreased to undetectable amounts by 72 h (Fig. 1a). We confirmed the specificity of NF- κ B activation by using unlabeled NF- κ B-binding DNA as a competitor to diminish the signal.

To determine NF- κ B activation in naive and memory CD4⁺ T cells, we stimulated enriched subsets of normal B6 CD44^{lo} (naive) and CD44^{hi} (memory) CD4⁺ T cells by TCR-CD28 ligation for 24 h, followed by EMSA to detect transcriptional activity of NF- κ B in the nuclear extracts; we used total CD4⁺ cells as a control. Nuclear translocation of NF- κ B was much more prominent for naive CD4⁺ cells than for memory cells; in contrast, transcriptional activity of an internal control (Oct-1) was the same for both subsets of CD4⁺ T cells (Fig. 1b).

To determine the extent of nuclear translocation of individual NF- κ B family members in each subset, we treated naive CD4⁺ T cells for 24 h with mAbs to TCR and CD28, then purified nuclear extracts and did immunoblot analysis with NF- κ B protein subunit-specific antibodies. Nuclear extracts had substantial amounts of both p50 and RelA, a small amount of c-Rel protein and a conspicuous absence of p52 or RelB proteins (Fig. 1c). Consistent with those findings, analysis of the nuclear extracts after incubation with antibodies specific for each NF- κ B protein subunit ('supershift assay') showed that the mobility shift of the NF- κ B DNA probe was greatest with anti-p50 or anti-RelA but only minimal with anti-p52 or anti-RelB (Fig. 1d), suggesting a predominance of p50-RelA dimers. That indicated, therefore, that early activation of NF- κ B in naive CD4⁺ cells reflects nuclear translocation of NF- κ B1 (p50)-RelA, with little or no contribution from NF- κ B2 (p52)-RelB.

NF- κ B2 in CD4⁺ T cell activation

The findings reported above failed to explain the T cell defects seen in NIK-deficient *aly/aly* and *Relb*^{-/-} mice^{13,20,29}. Total CD4⁺ T cells have been used in studies published before; thus, it was unclear whether the abnormalities noted occur at the level of specific CD4⁺ T cell subsets. To examine that issue, we compared the functions of total CD4⁺ cells and enriched subsets of naive and memory CD4⁺ cells. As anticipated from prior studies^{13,20,29}, the proliferative responses of total CD4⁺ cells treated for 3 d *in vitro* with mAbs to TCR and CD28 were much lower (50–70% reduction) for *Relb*^{-/-}, *aly/aly* and *Map3k14*^{-/-} mice than for heterozygous littermates or wild-type B6 mice (Fig. 2a). We obtained similar findings with mixed-lymphocyte reactions, in which proliferative responses were elicited by exposure to allogeneic (BALB/c) spleen cells (Fig. 2b). The decreased response of *Relb*^{-/-}, *aly/aly* and *Map3k14*^{-/-} CD4⁺ cells was only mildly improved after removal of CD25⁺CD4⁺ cells; that is, cells with T regulatory function (T_{reg} cells)^{35–37} (Fig. 2a–c). That finding was unexpected because removing CD25⁺ T_{reg} cells from control CD4⁺ cell samples, thus leaving CD25⁻CD4⁺ cells, led to enhanced responses (Fig. 2c, left versus right). Notably, CD25⁺CD4⁺ cells are nearly all CD44^{hi}, but about 50% of CD44^{hi} cells are CD25⁻. In wild-type mice, CD25⁻CD44^{hi}CD4⁺ cells have little or no T regulatory function and are generally considered to be memory (or 'memory-phenotype') cells. As shown for *aly/+* cells in Figure 2c, left, depleting normal control cell samples of both CD25⁺ and CD44^{hi} cells, thus leaving enriched naive CD25⁻CD44^{lo}CD4⁺ cells, led to much lower proliferative responses than those noted after removal of CD25⁺ cells alone. These findings indicated that in wild-type mice, total CD44^{hi} cells are a mixture of two functionally distinct populations: an inhibitory population of CD25⁺ T_{reg} cells, and a helper population of CD25⁻ T memory cells, which probably release stimulatory cytokines (discussed below). The situation with respect to these cell subtypes and functions is radically different for NIK-deficient cells.

For NIK-deficient *aly/aly* cells, poor TCR-mediated proliferative responses were generally improved only slightly after selective removal

of CD25⁺ cells (classical T_{reg} cells). In contrast, removal of both CD25⁺ and CD44^{hi} cells led to a substantial increase in the response; thus, the remaining CD25⁻CD44^{lo}CD4⁺ naive aly/aly T cells demonstrated a hyper-responsive proliferation compared with that of a comparable population of CD4⁺ cells from control mice (Fig. 2a,b,d versus Fig. 2d-f). We noted the hyper-responsiveness of CD44^{lo}CD4⁺ aly/aly cells in samples from *Map3k14*^{-/-} and *Relb*^{-/-} mice, and it was apparent for both mixed-lymphocyte reactions and TCR-CD28-induced proliferation (Supplementary Fig. 1 online). We also noted hyper-responsiveness for the main subset of CD44^{int} cells, which like CD44^{lo} cells are considered immunologically naive (that is, they have not experienced foreign antigen stimulation; Fig. 2f); in contrast, CD44^{hi}CD4⁺ cells were hypo-responsive compared with control cells (Fig. 2g and Supplementary Fig. 1). In these and all subsequent experiments, samples were enriched for 'memory' CD44^{hi} cells by removal of CD25⁺ cells (which included activated T cells as well as T_{reg} cells) and CD62L⁺ cells.

The main conclusion from the experiments reported above is that in contrast to wild-type control cells, naive CD4⁺ cells in NIK-deficient and *Relb*^{-/-} mice are poised to hyper-respond to TCR-mediated signals and the hyper-proliferative response is 'suppressed' by CD25⁺CD44^{hi} memory T cells (called 'CD44^{hi}CD4⁺ memory T cells' here) when total CD4⁺ T cells are assayed. As discussed below, the properties of CD44^{hi}CD4⁺ memory T cells in wild-type and aly/aly mice are very different: CD44^{hi}CD4⁺ memory T cells from wild-type mice function as helper T cells for primed naive cells, whereas CD44^{hi}CD4⁺ memory T cells from aly/aly mice function as 'suppressor' cells.

To quantitatively evaluate the suppressor function of aly/aly CD44^{hi}CD4⁺ memory T cells, we monitored the dilution of carboxy-fluorescein diacetate succinimidyl diester (CFSE) in naive CD44^{lo}CD4⁺ 'reporter' cells preincubated with the fluorescent dye. Early (48 h) proliferative responses of CFSE-labeled control (aly/+) CD44^{lo}CD4⁺ cells were appreciably enhanced by the addition of a similar number (5×10^4) of syngeneic aly/+ CD44^{hi}CD4⁺ memory T cells (Supplementary Fig. 2 online). In contrast, the proliferation of aly/aly CD44^{lo}CD4⁺ cells was reduced considerably by the addition of syngeneic aly/aly CD44^{hi}CD4⁺ memory T cells (Supplementary Fig. 2). We obtained similar results when we incubated CD44^{hi}CD4⁺ memory T cells from wild-type B6 or aly/aly mice (both Thy-1.2⁺) with CFSE-labeled CD44^{lo}CD4⁺ cells from B6.PL mice (Thy-1.1⁺; Supplementary Fig. 2). For CD44^{hi}CD4⁺ memory T cells from wild-type mice, the 'helper' effect of these cells correlated with increased IL-2 in the mixed cultures (Supplementary Fig. 2), presumably reflecting IL-2 synthesis by the added CD44^{hi}CD4⁺ memory T cells. In contrast, the inhibitory influence of aly/aly CD44^{hi}CD4⁺ memory T cells correlated with a decrease in IL-2 in the cultures (Supplementary Fig. 2). To directly test the function of IL-2 in this experimental situation, we

added exogenous IL-2 and found that it was sufficient to overcome the inhibitory effect of adding aly/aly CD44^{hi}CD4⁺ memory T cells (Supplementary Fig. 2).

Because the CD44^{hi}CD4⁺ memory T cell samples in the experiments reported above were depleted of typical CD25⁺ T_{reg} cells, the substantial suppressive influence of aly/aly CD25⁺CD44^{hi}CD4⁺ memory T cells was very unexpected. These cells could have had high expression of Foxp3, a transcription factor that in normal mice is selectively expressed mainly in CD25⁺ T_{reg} cells³⁸⁻⁴⁰. That was not the case, however, as we found that Foxp3 protein was undetectable in both wild-type and aly/aly CD25⁺CD44^{hi}CD4⁺ memory T cells even after TCR stimulation (Supplementary Fig. 3 online). Detection of Foxp3 protein was restricted to CD25⁺CD4⁺ typical T_{reg} cells, and the numbers of Foxp3⁺ cells were much lower (70-80% reduction) for aly/aly than for wild-type, consistent with published findings^{30,41}.

Mechanism of suppression

The findings reported above indicated that aly/aly naive and memory T cell subsets differ considerably in their capacity to synthesize and/or use IL-2. To test that hypothesis, we evaluated both cell subsets for IL-2 synthesis and IL-2R α (CD25) expression after TCR-CD28 ligation (Fig. 3). For naive CD4⁺ T cells, there was somewhat less IL-2, as measured by enzyme-linked immunosorbent assay (ELISA), in the

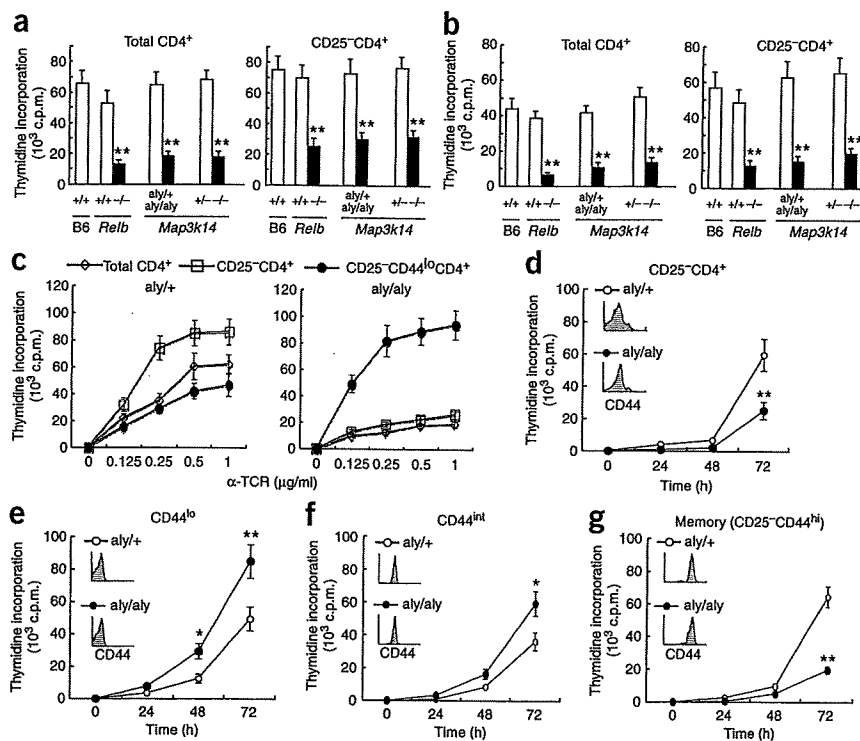


Figure 2 T cell responses of mice deficient in NF- κ B2-RelB. (a,b) Proliferation assays of total CD4⁺ and enriched CD25⁻CD4⁺ cell populations from spleens of *Relb*^{-/-}, aly/aly, NIK-deficient (*Map3k14*^{-/-}) and control (B6, *Relb*^{+/+}, aly/+ and *Map3k14*^{+/+}) mice stimulated for 72 h by TCR-CD28 ligation as in Figure 1 (a) or by culture for 96 h together with irradiated T cell-depleted spleen cell samples from BALB/c mice (b). (c) Proliferation assays of total, CD25⁻ and CD25⁻CD44^{lo} CD4⁺ T cells from aly/+ and aly/aly mice; cells were stimulated for 72 h with 0–1 μ g/ml (horizontal axes) of mAb to TCR (α -TCR) and 20 μ g/ml of mAb to CD28. (d–g) Proliferation assays of CD25⁻CD4⁺ cells and enriched subsets of CD44^{lo}, CD44^{int} and CD44^{hi} CD4⁺ T cells (all CD25⁻) separated by FACSsort and stimulated for 72 h with TCR-CD28 ligation. Insets, CD44 expression on the cells before culture. *, $P < 0.05$, and **, $P < 0.005$, aly/aly mice versus control mice. Data are means \pm s.d. of triplicate samples and are representative of three independent experiments.

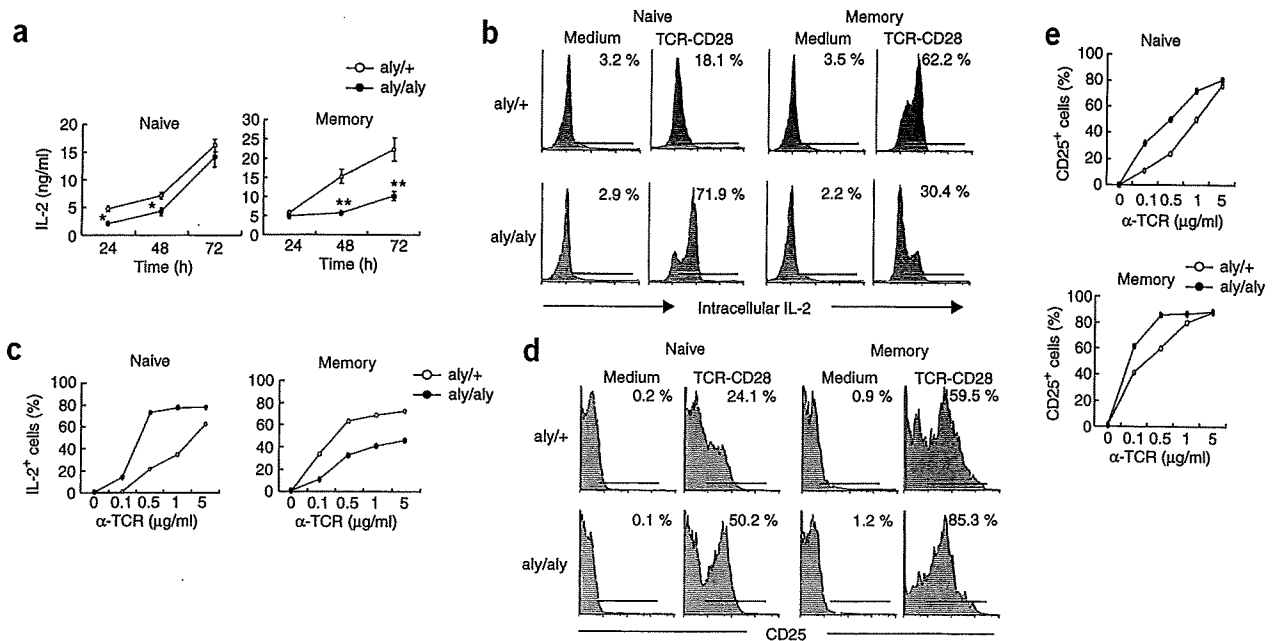


Figure 3 IL-2 secretion and IL-2R synthesis by aly/aly CD4⁺ subsets. (a) ELISA of IL-2 in culture supernatants of aly/aly and aly/+ naive CD44^{lo} and memory CD44^{hi}CD4⁺ T cells stimulated (time, horizontal axes) by TCR-CD28 ligation (as in Fig. 1a). Data are means \pm s.d. of triplicate samples and are representative of four independent experiments. *, $P < 0.05$, and **, $P < 0.005$, aly/aly mice versus control mice. (b,c) Flow cytometry for intracellular IL-2 in aly/aly and aly/+ naive CD44^{lo} and memory CD44^{hi}CD4⁺ T cells stimulated for 24 h with mAb to TCR (0.1–5 μ g/ml; horizontal axes) and mAb to CD28 (20 μ g/ml; 'TCR-CD28'). (b) Representative data for percent IL-2⁺ cells (numbers above horizontal lines, in top right corners) after stimulation at 0.5 μ g/ml of mAb TCR. (c) Mean percent of IL-2⁺ cells after stimulation with 'graded' concentrations of mAb to TCR. (d,e) Flow cytometry for CD25 expression on CD4⁺ T cells of aly/aly and aly/+ mice from b,c. (d) Numbers above horizontal lines indicate percent CD25⁺ cells after stimulation at 0.5 μ g/ml of mAb TCR. (e) Percent CD25⁺ cells after stimulation with 'graded' concentrations of mAb to TCR. Results are representative of three to five independent experiments.

culture supernatants of aly/aly cells than of wild-type (aly/+) cells (Fig. 3a). That result was unexpected given the enhanced proliferative responses of naive aly/aly cells; however, intracellular staining showed that there was much more IL-2 protein in the cytoplasm of aly/aly cells than wild-type cells (Fig. 3b,c). Likewise, induction of CD25 cell surface expression was much greater on aly/aly cells than on wild-type cells (Fig. 3d,e). Hence, the reduced IL-2 in the culture supernatants of naive aly/aly cells presumably reflected enhanced IL-2 consumption through binding to the increased CD25 expressed on the cell surface. From these results we concluded that the increased proliferative responses of aly/aly naive cells correlated with increased IL-2 and IL-2R protein synthesis.

For CD44^{hi}CD4⁺ memory T cells, there was much less IL-2 synthesis in cells from aly/aly mice than in cells from control (aly/+) mice, as assessed by both the amount of IL-2 secreted into the culture supernatant (Fig. 3a) and the amount detected inside the cells by intracellular staining (Fig. 3b,c). However, the results were very different for IL-2R; compared with wild-type CD44^{hi}CD4⁺ memory T cells, aly/aly CD44^{hi}CD4⁺ memory T cells had enhanced CD25 cell surface expression, similar to that seen in the aly/aly naive cells (Fig. 3d,e), and the cells also demonstrated enhanced CD69 expression (data not shown). Hence, the reduced proliferative response of aly/aly CD44^{hi}CD4⁺ memory T cells correlated with poor IL-2 synthesis despite high IL-2R induction. The suppressive effect of aly/aly CD44^{hi}CD4⁺ memory T cells on naive CD4⁺ T cells therefore might reflect the possibility that aly/aly CD44^{hi}CD4⁺ memory T cells deplete the cultures of IL-2 because of enhanced expression of CD25. In agreement with that interpretation, proliferative responses of both wild-type and aly/aly naive CD4⁺ cells were considerably reduced by

depleting the cultures of IL-2 with mAb to IL-2 (Supplementary Fig. 2). Moreover, in mixed cultures of naive and memory CD4⁺ T cells (Supplementary Fig. 2), poor IL-2 synthesis by these cells combined with high IL-2R expression led to IL-2 depletion, which is the likely mechanistic explanation of the suppressive property of aly/aly memory cells.

The finding that total aly/aly CD4⁺ cells were hypo-responsive to TCR-CD28 ligation after selective depletion of CD25⁺ cells suggested that the CD25⁺ T_{reg} cells in aly/aly mice are functionally defective. Alternatively, the aly/aly T_{reg} cells might have 'normal' suppressive activity but function poorly because their relative numbers are much lower than those in wild-type mice (Supplementary Fig. 3). In support of the last idea, the capacity of purified CD25⁺CD4⁺ cells to suppress proliferation of wild-type naive CD4⁺ T cells was almost as efficient for aly/aly CD25⁺ cells as it was for wild-type CD25⁺ cells (Supplementary Fig. 4 online). Likewise, aly/aly and wild-type CD25⁺ cells were comparable in their low synthesis of IL-2 but high synthesis of both IL-10 and transforming growth factor- β (Supplementary Fig. 4).

In vivo responses

To examine responses *in vivo*, we first compared normal and aly/aly CD4⁺ subsets for their capacity to undergo homeostatic proliferation in syngeneic irradiated mice. As described before⁴², the paucity of T cells in irradiated mice allows adoptively transferred CD4⁺ T cells to proliferate in response to major histocompatibility complex class II-restricted self peptides. Homeostatic proliferation of CFSE-labeled naive CD44^{lo}CD4⁺ cells was greater for aly/aly cells than for normal aly/+ cells (Fig. 4a). In contrast, homeostatic proliferation

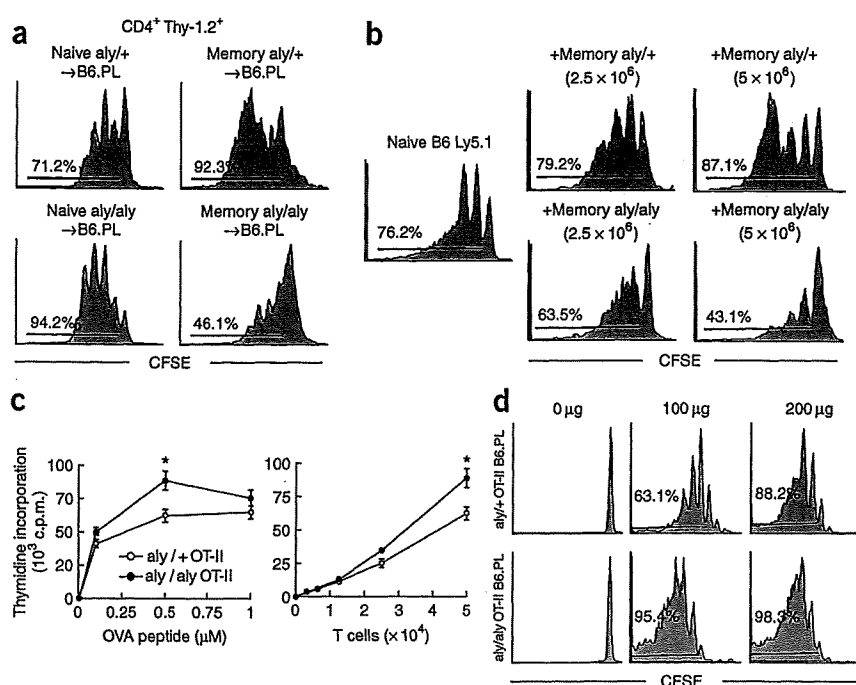


Figure 4 Proliferative responses of naive and memory *aly/aly* CD4⁺ subsets *in vivo*. (a) Flow cytometry of CFSE-labeled naive CD44^{lo} or memory CD44^{hi} CD4⁺ T cells (5×10^6) from *aly/aly* and *aly/+* mice (both Thy-1.2) transferred 7 d previously into irradiated (700 rads) B6.PL (Thy-1.1) mice. (b) Flow cytometry of CFSE-labeled naive CD4⁺ T cells (5×10^6) from B6 Ly5.1 mice transferred together with unlabeled *aly/+* or *aly/aly* memory cells (2.5×10^6 or 5×10^6 ; both Ly5.2) into irradiated (700 rads) B6 mice. Ly5.1⁺CD4⁺ T splenocytes were evaluated 7 d after transfer. (c) Proliferative assay of naive CD44^{lo}CD4⁺ T cells from either *aly/aly* OT-II or *aly/+* OT-II mice cultured for 72 h *in vitro* with irradiated (1,500 cGy) T cell-depleted B6 spleen cell samples (5×10^5 cells) in the presence of 'graded' concentrations of OVA peptide (left) or with 'graded' numbers of T cells and 0.5 μ M OVA peptide (right). Data are means \pm s.d. of triplicate cultures. *, $P < 0.05$, *aly/aly* OT-II versus *aly/+* OT-II cells. (d) Flow cytometry of CFSE-labeled naive CD4⁺ T cells (5×10^6) from *aly/aly* or *aly/+* OT-II B6.PL mice (both Thy-1.1⁺) transferred intravenously into B6 (Thy-1.2⁺) mice; 1 d later, OVA peptide (0–200 μ g) was injected intraperitoneally into recipient mice. Thy-1.1⁺V β 5.2⁺CD4⁺ T splenocytes were analyzed 3 d after peptide injection. Numbers above horizontal lines (a,b,d) indicate percentages of divided cells from the fourth division. Results are representative of two (b) or three (a,c,d) independent experiments.

of CD44^{hi}CD4⁺ memory T cells was much less for *aly/aly* cells than for normal *aly/+* cells. Likewise, homeostatic proliferation of wild-type naive CD4⁺ cells (CFSE labeled) *in vivo* was enhanced by the addition of wild-type memory CD4⁺ cells (not CFSE labeled) but was inhibited by the addition of *aly/aly* CD44^{hi}CD4⁺ memory T cells (Fig. 4b). There was also hyper-responsiveness of naive *aly/aly* CD4⁺ cells *in vivo* for antigen-specific CD4⁺ cells. Thus, compared with control *aly/+* naive OT-II cells, *aly/aly* naive CD44^{lo}CD4⁺ OT-II cells demonstrated enhanced proliferative responses to stimulation with specific ovalbumin (OVA) peptide *in vitro* (Fig. 4c) and to a limiting dose of OVA peptide (100 μ g/mouse) *in vivo* (Fig. 4d).

NF- κ B expression in naive versus memory CD4⁺ cells

To understand the hyper-responsiveness of naive *aly/aly* cells, it was important to determine the expression of individual NF- κ B subunits in wild-type and NIK-deficient CD4⁺ cells. For naive CD44^{lo}CD4⁺ cells from control *aly/+* mice, confocal microscopy after TCR-CD28 ligation for 24 h showed increased synthesis of NF- κ B1 and RelA in the cytoplasm and translocation of both subunits to the nucleus (Fig. 5a); the two subunits were in close proximity, as indicated by

their merged fluorescence. We obtained similar results for naive *aly/aly* cells, although in this case the fluorescence of NF- κ B1 and RelA was stronger in the nucleus than in the cytoplasm, suggesting increased nuclear translocation (Fig. 5a). In support of that conclusion, immunoblot analysis of nuclear extracts showed substantially more p50 and RelA in *aly/aly* cells than in *aly/+* cells (Fig. 5b). In contrast, NF- κ B2 and RelB were almost undetectable in the nuclei of both *aly/aly* and *aly/+* cells, despite high expression of both proteins in the cytoplasm of *aly/+* cells (Fig. 5a). These data confirmed that at 1 d after TCR-CD28 ligation, nuclear translocation of NF- κ B was restricted mainly to NF- κ B1 (p50)–RelA dimers (Fig. 1). There was also enhanced nuclear translocation of p50 and RelA in naive *Relb*^{-/-} cells, as demonstrated by both confocal and immunoblot analyses (Supplementary Fig. 5 online). Thus, hyper-responsiveness of naive *aly/aly* and *Relb*^{-/-} CD4⁺ T cells correlated with increased nuclear translocation of NF- κ B1 (p50)–RelA compared with that of wild-type naive T cells.

Through I κ B-like ankyrin repeats, NF- κ B2 p100 can bind other NF- κ B family members and thereby prevent their nuclear translocation³. The hyper-responsiveness of naive *aly/aly* CD4⁺ cells, therefore, might reflect reduced p100. To test that possibility, we evaluated cytoplasmic and total cell lysates of naive *aly/aly* CD4⁺ cells; both showed a substantial reduction in p100 protein relative to that in *aly/+* cells (Fig. 5c). We confirmed that result by fluorescence resonance energy transfer (FRET) analysis, which showed that association of p52-p100 with RelA or p50 in *aly/aly* cells was undetectable (Fig. 5d). In contrast, control naive *aly/+* cells showed substantial intracytoplasmic association of p52-p100 with both RelA and p50 (Fig. 5d). For the control *aly/+* and wild-type B6 cells, we confirmed the association of RelA and p50 with p52-p100 by immunoprecipitation of cytoplasmic extracts with anti-p52-p100 followed by immunoblot with NF- κ B subunit-specific antibodies. After TCR-CD28 stimulation, p52-p100 protein (mostly p100) was associated with RelB, RelA and p50 but not with c-Rel (Fig. 5e and Supplementary Fig. 5). Also, immunoprecipitation of [³⁵S]methionine-labeled cells with anti-RelA demonstrated a notable p100-RelA complex in wild-type cells but not in *aly/aly* cells (Supplementary Fig. 5). Based on those observations, the hyper-responsiveness of naive *aly/aly* CD4⁺ cells can be attributed to reduced p100, which enhances nuclear translocation of p50-RelA and NF- κ B-mediated gene transcription and cell activation.

For *aly/+* CD44^{hi}CD4⁺ memory T cells, there was increased production and nuclear translocation of both NF- κ B1 and RelA after TCR-CD28 ligation, although less than for naive *aly/+* cells (Fig. 5a). Nuclear translocation of the alternative NF- κ B2 and RelB proteins was very prominent for *aly/+* CD44^{hi}CD4⁺ memory T cells and correlated with much more p52 in total cell lysates (Fig. 5c). In notable contrast, *aly/aly* CD44^{hi}CD4⁺ memory

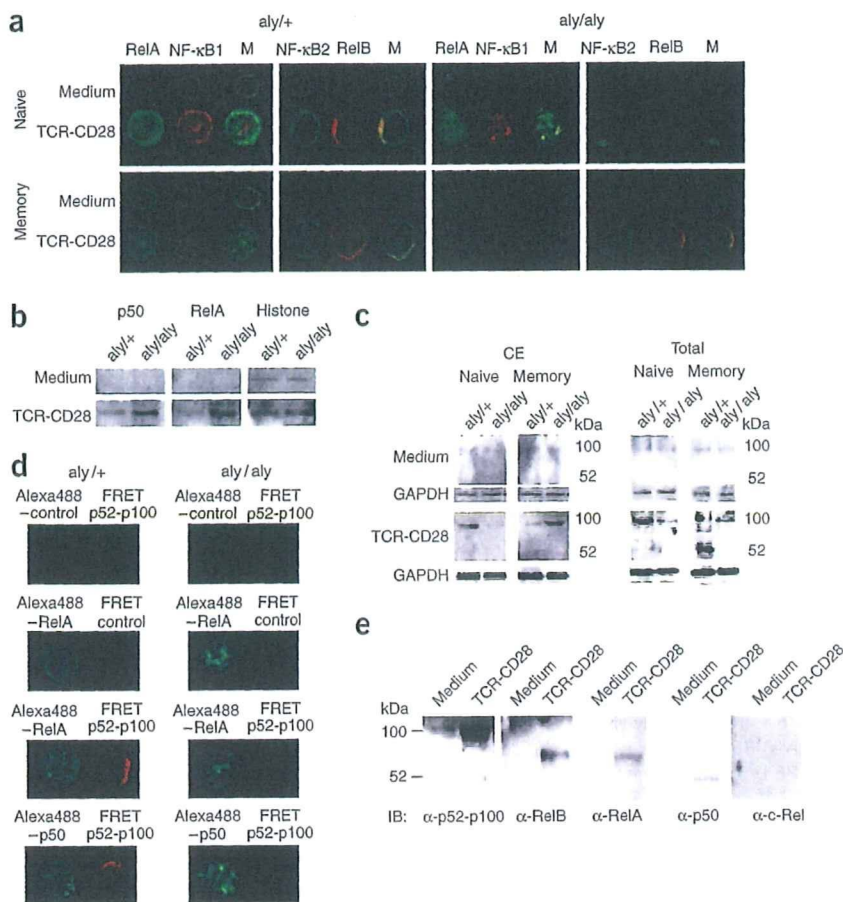


Figure 5 Molecular interactions between NF-κB subunits during T cell activation. **(a)** Confocal microscopy of naive CD44^{lo} and memory CD4⁺ T cells from aly/aly and aly/+ mice stimulated for 24 h with TCR-CD28 ligation (as in Fig. 1), fixed in 3% paraformaldehyde on a glass slide and stained with anti-p50, anti-RelA, anti-p52 and anti-RelB followed by Alexa Fluor 488-labeled (green) or Alexa Fluor 568-labeled (red) anti-mouse or anti-rabbit IgG. M, merged image. Original magnification, ×630. **(b)** Immunoblot to detect p50 and RelA in nuclear extracts from naive aly/aly and aly/+ CD4⁺ T cells after 24 h of TCR-CD28 ligation. Histone serves as a control. **(c)** Immunoblot to detect NF-κB2 (p52-p100) in total and cytosolic extracts (CE) of stimulated naive and memory CD4⁺ T cells from aly/aly and aly/+ mice. Glyceraldehyde phosphate dehydrogenase (GAPDH) serves as a control. **(d)** FRET analysis of aly/aly and aly/+ naive CD4⁺ T cells stimulated for 24 h with TCR-CD28 ligation, fixed in 3% paraformaldehyde on a glass slide and stained with Alexa Fluor 488-labeled (Alexa488) anti-p50 or anti-RelA and Alexa Fluor 546-labeled anti-p52. The binding of p52 to RelA or p50 is detected as a FRET signal (red). Control, no first antibody. Original magnification, ×630. **(e)** Immunoprecipitation with anti-NF-κB2 p100-p52 and immunoblot (IB) for p100-p52, RelB, p50, RelA and c-Rel in cytosolic extracts of naive B6 CD4⁺ T cells stimulated for 24 h with TCR-CD28 ligation. Results are representative of three to five independent experiments.

T cells demonstrated no detectable nuclear translocation of RelA, NF-κB1, NF-κB2 or RelB (Fig. 5a). For NF-κB2, p100 was apparent in the cytoplasm of aly/aly CD44^{hi}CD4⁺ memory T cells, as shown by both confocal microscopy (Fig. 5a) and immunoblot of cytoplasmic extracts (Fig. 5c); processing of p100 to p52 was undetectable.

Kinetics of p100 synthesis and p52 nuclear translocation

The data reported above apply to early (day-1) responses to TCR-CD28. For naive aly/aly CD4⁺ cells, kinetics experiments showed that p100 in protein cytoplasmic extracts was undetectable for up to 72 h, which correlated with above-normal nuclear translocation of NF-κB1-p50 throughout this time (Fig. 6a,b). In contrast, for aly/+ naive CD4⁺ cells, the amount of p100 in cytoplasmic extracts was high at 24 and 48 h, which correlated with only moderate amounts of NF-κB1-p50 in nuclear extracts. We also noted that nuclear p50 in aly/+ naive cells fell to undetectable amounts by 72 h and was 'replaced' by low but detectable amounts of p52-RelB. We noted the delayed nuclear translocation of p52-RelB only for aly/+ and not aly/aly cells, and this paralleled a decrease in cytoplasmic p100, perhaps reflecting p100-to-p52 processing; delayed nuclear translocation of p52-RelB in aly/+ cells was also apparent by confocal microscopy (Fig. 6c). These observations strengthen the view that via direct protein-protein interaction, p100 in the cytoplasm serves to inhibit nuclear translocation of p50-RelA in aly/+ naive CD4⁺ cells and thereby acts as a 'brake' for gene transcription. The data also indicate that after several days, NF-κB activation in aly/+ naive CD4⁺ cells involves a 'switch' from NF-κB1- to NF-κB2-dependent pathways.

Induction of autoimmune disease

NIK-deficient and *Relb*^{-/-} mice develop CD4-dependent, slow-onset (> 14 weeks), multiorgan autoimmune disease, which can be 'adoptively transferred' to hosts deficient in recombination-activating gene 2 (*Rag2*^{-/-} hosts)^{20,31,32}. Given the data reported above, autoimmune disease might be enhanced by the removal of CD44^{hi}CD4⁺ memory T cells. To investigate that possibility, we adoptively transferred enriched subsets of aly/+ and aly/aly CD4⁺ T cells into *Rag2*^{-/-} hosts. For both control naive and memory aly/+ CD4⁺ T cells, cell numbers recovered from the spleen after adoptive transfer were modest (about 5 × 10⁵ cells/mouse; Fig. 7a), infiltration of lymphocytes in the lungs and lacrimal glands was minimal (Fig. 7b) and evidence of autoimmune disease in those tissues was undetectable (Fig. 7c). We obtained very different results after injecting aly/aly CD4⁺ cells. For those, injection of either total CD4⁺ or CD25⁻CD4⁺ cells resulted in relatively low recovery of cells from the spleen (Fig. 7c), thus correlating with the hypo-responsiveness of the aly/aly cells (as demonstrated above). As for autoimmune disease induction, both populations produced mild but detectable lymphocyte infiltration of lungs and lacrimal glands, with such pathology being slightly more prominent with CD25⁻ cells (Fig. 7b,c). The effects were much more prominent, however, after injection of enriched naive CD4⁺ cells (that is, samples depleted of both T_{reg} cells and memory CD4⁺ T cells): cell recoveries were considerably enhanced in the spleen (presumably reflecting enhanced homeostatic proliferation) and there was substantial lymphocytic infiltration and prominent pathology in lung and lacrimal glands. These results demonstrated that the hyper-responsiveness of purified naive aly/aly CD4⁺ cells applies not only to short-term proliferative

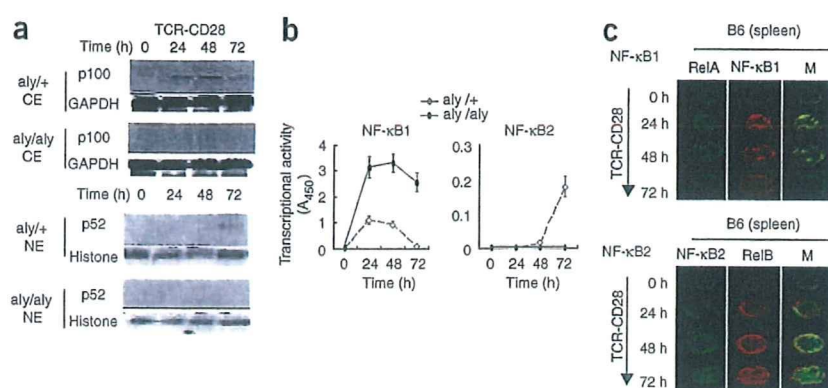


Figure 6 Kinetics of NF- κ B1 and NF- κ B2 expression in naive CD4⁺ cells after TCR ligation. (a) Immunoblot to detect p100 and p52 in cytosolic extracts (CE) and nuclear extracts (NE) of aly^{+/+} and aly/aly naive CD4⁺ cells after 0–72 h of TCR-CD28 ligation. GAPDH and histone serve as controls. Results are representative of two independent experiments. (b) Nuclear expression of NF- κ B1 and NF- κ B2. Relative activities were measured with the nuclear extracts of naive T cells from aly^{+/+} and aly/aly mice stimulated for 0–72 h with TCR-CD28 ligation. Data represent means \pm s.d. of triplicate wells. (c) Confocal analysis of NF- κ B subunits in naive CD4⁺ cells from B6 mice stimulated for 0–72 h with TCR-CD28 and then stained with anti-p50, anti-RelA, anti-p52 and anti-RelB, followed by secondary Alexa Fluor 488-labeled (green) or Alexa Fluor 568-labeled (red) anti-mouse or anti-rabbit IgG. M, merged images. Original magnification, \times 630. Results are representative of two independent experiments.

responses and related cytokine production but also to induction of autoimmune disease after transfer into *Rag2*^{-/-} hosts.

DISCUSSION

For T cells, primary immune responses generally require the classical NF- κ B1 pathway⁴³; whether T cell activation also requires the non-classical NF- κ B2 pathway is less clear. Nevertheless, studies of NIK-deficient aly/aly mice have led to the conclusion that ‘optimal’

activation of mature T cells requires signaling via NIK as well as PKC- θ ¹³. Because NIK controls processing of p100 to p52, it would seem to follow that T cell activation is partly dependent on nonclassical NF- κ B2. However, the T cell defects in aly/aly mice also correlate with reduced spleen cell expression of p50, RelA and c-Rel^{13,29}, suggesting an indirect effect on the classical NF- κ B1 pathway.

Here we have shown that the relative contributions of NF- κ B1 and NF- κ B2 to T cell activation are crucially dependent on whether the cells are immunologically naive. We have made two main points in this context. The poor immune response of total aly/aly T cells (equally true for NIK-deficient *Map3k14*^{-/-} and *Relb*^{-/-} cells) does not reflect a positive requirement for NF- κ B2 but instead reflects the inhibitory function of a unique population of ‘suppressor’ cells in the total cell population. However, when depleted of those suppressor cells, the aly/aly naive T cell samples showed their cell-intrinsic ‘defect’ of hyper-reactivity after TCR stimulation. Thus, the aly, NIK-deficient and *Relb*^{-/-} phenotype is actually a combination of a cell-extrinsic suppressor function in a subset of CD44^{hi}CD4⁺ NIK-deficient T cells and a cell-intrinsic hyperactivation response in naive CD4⁺ T cells that lack NIK function.

For wild-type mice, it is well established that primary responses of T cells can be suppressed by a population of CD25⁺Foxp3⁺CD4⁺ T_{reg} cells and are enhanced when T_{reg} cells are eliminated^{38–40}. For aly/aly T cells, the enhancing effect of removing CD25⁺CD4⁺ T_{reg} cells was much less pronounced, probably because the proportion of the NIK-deficient CD25⁺CD4⁺ T_{reg} cells (specifically Foxp3⁺ cells) is only 20–30% of the number of such cells in wild-type mice. However, the aly/aly CD25⁺CD4⁺ T_{reg} cells are suppressor cells functionally, as after enrichment they suppressed the proliferation of naive T cells nearly as well as T_{reg} cells from control mice. In addition, cytokine production by T_{reg} cells from aly/aly and control mice was comparable. Hence, except for an overall reduction in

induction of autoimmune disease by subsets of aly/aly and aly/aly CD4⁺ cells. Enriched subsets of total CD4⁺, CD25⁺CD4⁺ or naive (CD25⁻CD44^{lo}) CD4⁺ cells from aly/aly and aly/aly mice were transferred into *Rag2*^{-/-} hosts (5×10^6 cells/mouse); mice were killed 4 weeks after transfer. (a) Total number of CD3⁺CD4⁺ splenocytes. Data are means \pm s.d. of four to five mice. *, $P < 0.05$, and **, $P < 0.005$, aly/aly versus aly/aly cells in each group. (b) Histopathological analysis of lung and lacrimal gland sections. Left, number of lymphocytes/mm² of lung; right, pathological score of inflammatory lesions of lacrimal glands. Data are means \pm s.d. of four to five mice. (c) Histology of lungs and lacrimal gland sections stained with hematoxylin and eosin. Original magnification, \times 100. Results are representative of four to five mice in each group.

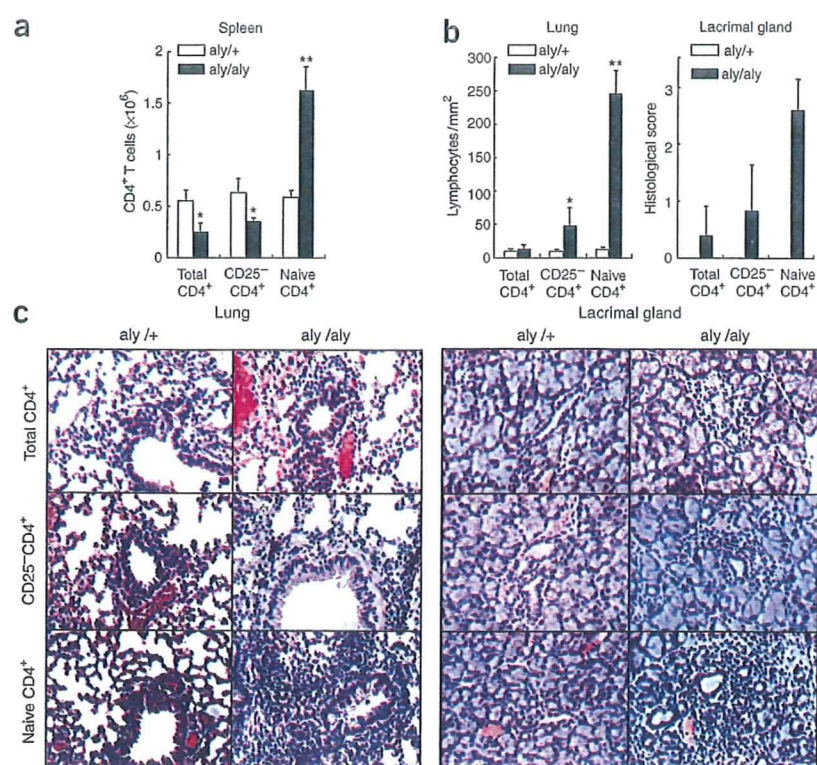


Figure 7 Induction of autoimmune disease by subsets of aly/aly and aly/aly CD4⁺ cells. Enriched subsets of total CD4⁺, CD25⁺CD4⁺ or naive (CD25⁻CD44^{lo}) CD4⁺ cells from aly/aly and aly/aly mice were transferred into *Rag2*^{-/-} hosts (5×10^6 cells/mouse); mice were killed 4 weeks after transfer. (a) Total number of CD3⁺CD4⁺ splenocytes. Data are means \pm s.d. of four to five mice. *, $P < 0.05$, and **, $P < 0.005$, aly/aly versus aly/aly cells in each group. (b) Histopathological analysis of lung and lacrimal gland sections. Left, number of lymphocytes/mm² of lung; right, pathological score of inflammatory lesions of lacrimal glands. Data are means \pm s.d. of four to five mice. (c) Histology of lungs and lacrimal gland sections stained with hematoxylin and eosin. Original magnification, \times 100. Results are representative of four to five mice in each group.

total numbers, the 'classical' CD25⁺CD4⁺ T_{reg} cells in *aly/aly* mice showed no obvious abnormality.

The situation with memory CD4⁺ cells was very different. Wild-type memory CD25⁺CD44^{hi}CD4⁺ T cells functioned like 'typical' antigen-primed T cells: they rapidly generated large amounts of IL-2 after TCR ligation *in vitro* and provided efficient help to naive CD4⁺ T cells. In contrast, all of the data presented here indicate the conclusion that *aly/aly* memory CD4⁺ T cells function as suppressor cells. In every test, both *in vivo* and *in vitro*, elimination of both CD25⁺ ('typical' T_{reg} cells) and CD25⁻CD44^{hi}CD4⁺ memory T cells was required for reversal of the poor proliferative response of *aly/aly* CD4⁺ cells. The origin of such 'naturally' occurring CD44^{hi}CD4⁺ memory cells in either wild-type or NIK-deficient mice is unclear; such cells may arise through contact with various environmental antigens and/or be stimulated by self antigens.

The mechanism of suppression by *aly/aly* memory CD4⁺ cells has yet to be resolved. After TCR ligation, suppression correlated with a combination of low IL-2 synthesis and enhanced CD25 expression, which suggests that the cells could function mostly through CD25-mediated consumption of IL-2. That idea fits with the finding that suppression by *aly/aly* memory CD4⁺ T cells *in vitro* could be overcome by the addition of exogenous IL-2. However, simple consumption of IL-2 is unlikely to explain the strong inhibitory influence of *aly/aly* memory CD4⁺ T cells *in vivo*, which was apparent for both homeostatic proliferation and autoimmune disease induction. By analogy with 'typical' T_{reg} cells, suppression via transforming growth factor- β or IL-10 production could be involved³⁵⁻³⁷; however, at least *in vitro*, production of these cytokines was no higher for *aly/aly* memory CD4⁺ T cells than for control memory cells. Hence, resolving the mechanisms of suppression by *aly/aly* memory CD4⁺ cells must await further investigation.

Why memory CD4⁺ cells in *aly/aly* mice show strong CD25 expression but poor IL-2 synthesis after TCR stimulation is also still unclear. Nevertheless, it is notable that despite enhanced synthesis of CD25, *aly/aly* memory CD4⁺ T cells demonstrated very little nuclear translocation of p50, RelA, p52, RelB (as presented here) or c-Rel (data not shown), indicating that CD25 upregulation in *aly/aly* memory cells involves an NF- κ B-independent pathway, such as AP-1 and/or NF-AT^{44,45}. Because nuclear translocation of p50-RelA was high in naive *aly/aly* T cells, the limited translocation of these subunits in memory *aly/aly* T cells in comparison was unexpected although consistent with the reduced p50 and RelA reported for *aly/aly* total spleen cells²⁹. Based on those preliminary data, poor nuclear translocation of p50 and RelA in memory *aly/aly* CD4⁺ cells correlates with reduced synthesis in the cytoplasm, suggesting that p50 and RelA synthesis in memory CD4⁺ cells is partly controlled by a NIK-dependent pathway. In addition, as in stimulated osteoclast precursors²⁶, the low amounts of p50 and RelA in *aly/aly* memory CD4⁺ cells may be 'held' in the cytoplasm through association with p100; thus, cytoplasmic p100 in *aly/aly* cells is much higher in memory cells than naive cells.

The hyper-responsiveness of naive *aly/aly* CD4⁺ cells was associated with increased synthesis of both IL-2R (CD25) and IL-2, relative to that of wild-type naive cells; detection of an increase in IL-2 synthesis required intracellular staining, presumably because of efficient absorption of extracellular IL-2 by the increased CD25 expressed on the cell surface. Other signs of T cell activation, such as CD69 expression and interferon- γ synthesis, were nearly normal (data not shown), indicating that the hyper-responsiveness was centered on the IL-2-IL-2R axis. As for NF- κ B, it is particularly notable that the increased proliferative responses of naive *aly/aly* CD4⁺ cells were associated with considerable

increases in nuclear translocation of p50 and RelA, apparent in both nuclear extracts and by confocal microscopy. Therefore, this indicates that NIK functions by preventing nuclear translocation of p50 and RelA. The simplest possibility is that NIK regulates autocrine synthesis of p100 through continuous p100-p52 processing, thus allowing nuclear translocation of p52-RelB dimers and transcription of the gene encoding p100 (ref. 26); steady-state production of p100 then keeps p50 and RelA in the cytoplasm. We favor that hypothesis because there was much less p100 in *aly/aly* naive cells than in control cells; that result was also confirmed by FRET analysis, which showed no apparent association of p100 with p50 or RelA. Hence, we attribute the hyper-responsiveness of *aly/aly* naive CD4⁺ cells (as well as *Map3k14*^{-/-} (NIK-deficient) and *Relb*^{-/-} cells) to reduced p100 synthesis, which leads to unregulated nuclear translocation of p50-RelA and enhanced IL-2 and IL-2R synthesis. For *Relb*^{-/-} cells, p100 was also reduced (data not shown), presumably because expression of the gene encoding autocrine p100 is controlled by p52-RelB heterodimers²⁶.

For naive CD4⁺ cells from wild-type mice, despite prominent synthesis in the cytoplasm, nuclear translocation of p52-RelB was undetectable within the first 2 d after TCR-CD28-induced activation, indicating no involvement of the nonclassical NF- κ B2 pathway. However, by day 3 after TCR ligation, substantial nuclear translocation of p52-RelB was evident, which paralleled a decrease in p50-RelA. That result provides direct support for the hypothesis that NF- κ B2-RelB is involved in the later stages of the primary response⁴⁶⁻⁴⁸, perhaps by 'substituting' for the classical NF- κ B1 pathway. One point to emphasize here is that nuclear translocation of NF- κ B2-RelB presumably has only a positive effect on gene transcription and thus cannot account for the regulatory effect of NIK on TCR responsiveness. As mentioned above, we envisage that NIK acts as a 'brake' for the NF- κ B1 pathway simply by maintaining unprocessed p100 in the cytoplasm, thereby impeding entry of p50-RelA into the nucleus.

In summary, our data here have shown that the T cell defects reported for NIK-deficient mice¹³ and *Relb*^{-/-} mice²⁰ reflect a dominant form of immunoregulation in which otherwise hyper-responsive NIK-deficient naive T cells are suppressed by a subset of NIK-deficient CD25⁻ memory T cells. Only when the suppressor cells are eliminated is the cell-intrinsic phenotype of NIK-deficiency demonstrated. At face value, these results may seem at odds with the observation that *aly/aly* mice develop multiorgan autoimmune disease. That syndrome, associated with a reduction in classic CD25⁺ T_{reg} cells, may be triggered by poor negative selection in the thymus because of reduced expression of various self antigens in the thymic medulla³⁰. Given such a self-tolerance defect, it is unexpected that autoimmune disease in *aly/aly* mice is relatively mild, which suggests that the 'nontolerant' T cells in these mice are generally very well controlled, perhaps by the inhibitory memory subset we have described here. The fulminating autoimmune disease seen when purified naive *aly/aly* CD4⁺ cells were transferred adoptively is consistent with that idea.

METHODS

Mice. B6 and 129 mice were obtained from the Jackson Laboratory. *Map3k14*^{-/-} (NIK-deficient), *Map3k14*^{aly/aly} (*aly/aly*) and *Relb*^{-/-} mice were provided by R. Ulevitch (The Scripps Research Institute, La Jolla, California) and M. Kronenberg (La Jolla Institute for Allergy and Immunology, San Diego, California), and OT-II mice⁴⁹ (C57BL/6-Tg(TcraTcrb)425Cbn/J) were obtained from S. Webb (The Scripps Research Institute, La Jolla, California); *aly/aly* OT-II mice were generated by crossing of *aly/aly* mice with OT-II mice. *Rag2*^{-/-} mice were obtained from Taconic. All mice were maintained in specific pathogen-free conditions in our animal facility and the experiments were approved by an animal ethics board of The Scripps Research Institute (La Jolla, California) or Tokushima University (Tokushima, Japan).

Antibodies. Antibodies specific for p50 (C-19, NLS and D-17), p52 (K-27 and C-5), RelA (A-20, C-20 and F-6), RelB (C-19), c-Rel, histone and glyceraldehyde phosphate dehydrogenase were purchased from Santa Cruz Biotechnology and were used for immunoprecipitation, immunoblot analysis, EMSA and confocal microscopy.

Cell purification. For purification of CD4⁺ subsets, lymph node or spleen cells were treated for 45 min at 37 °C with cytotoxic mAbs specific for CD8 (3.168.8) and CD24 (J11D) plus guinea pig complement (Rockland)⁵⁰. After being washed, CD25⁺CD4⁺ T cells, NK1.1⁺ T cells and cells positive for major histocompatibility complex class II first underwent depletion by negative selection with DynaBeads (Dyna). Samples were enriched for CD44^{lo} and CD44^{hi} cells by negative selection with anti-CD44 (IM7) or anti-CD62L (Mel-14) and were positively 'panned' with anti-CD4 (RL172). In addition, samples were enriched for CD44^{lo}, CD44^{int} and CD44^{hi} CD4⁺ and CD25⁺CD4⁺ T cells by cell sorting with a FACSvantage (Becton Dickinson).

Culture conditions. Cells were cultured in 0.2 ml of RPMI medium supplemented with 50 μM 2-mercaptoethanol, L-glutamine and 10% FCS in 96-well tissue culture plates coated with mAbs specific for TCRβ (H57-597) and CD28 (37.51; eBiosciences).

Flow cytometry. A FACSort (Becton Dickinson) was used for flow cytometry and data were analyzed with FlowJo FACS Analysis software (Tree Star). Analysis of cell division with CFSE (Molecular Probes)⁴², intracellular cytokine production (IL-2) with a BD Cytofix/Cytoperm kit (BD Biosciences)⁵¹ and intracellular Foxp3 expression with an Intracellular Foxp3 Detection Kit (eBioscience) was done according to the manufacturers' instructions.

Proliferation assay. Cell proliferation was evaluated by [³H]thymidine incorporation or by counting of divisions by CFSE dilution of labeled cells. In most experiments, 5 × 10⁴ enriched CD4⁺ T cells were stimulated for 24–72 h with plate-bound mAbs to TCR (0.1–1 μg/ml) and CD28 (20 μg/ml). OT-II T cells (0.625 × 10⁴ to 5 × 10⁴ cells/well) were cultured together with irradiated (3,000 cGy) Thy-1.2⁺-depleted syngeneic spleen cell samples (5 × 10⁵ cells) and were stimulated with OVA peptide, amino acids 323–339 (Sigma Genosys). Stimulated cells were then pulsed with 0.5 μCi [³H]thymidine per well for the last 8 h of culture. For CFSE labeling, purified CD4⁺ T cells were resuspended with 0.1% BSA in PBS at a density of 5 × 10⁶ cells/ml and were labeled for 10 min at 37 °C with 0.3 μM CFSE. CFSE-labeled cells were 'quenched' with PBS containing 5% FCS and were washed twice. Cell division at 48–72 h was analyzed by flow cytometry.

EMSA. Nuclear extracts of stimulated CD4⁺ T cells were prepared as described⁵². Cells were washed twice with PBS and were resuspended in 100 μl ice-cold lysis buffer, were vortexed and were centrifuged for 5 min at 5,000g. Nuclear pellets were resuspended in 100 μl extraction buffer containing 20 mM HEPES, 1.5 mM MgCl₂, 0.2 mM EDTA, 0.4 mM NaCl, 2.5% glycerol and a mixture of protease inhibitors. After centrifugation for 30 min at 12,000g, nuclear extracts (0.5–5 μg) in the supernatant were incubated for 20 min at 25 °C with biotin-labeled κB oligonucleotide probe (5'-AGTTGAGGG GACTTCCCAGGC-3') and Oct-1 oligonucleotide probe (5'-TGTCGAATG CAAATCACTAGAA-3'). Protein-DNA complexes were resolved by nondenaturing 4–6% PAGE in 0.5× TBE and were transferred to nylon membranes (Pierce). After crosslinking of transferred DNA to the membranes, biotin-labeled DNA was detected with a LightShift Chemiluminescent EMSA Kit (Pierce) according to the manufacturer's instructions. For supershift assay, NF-κB subunit-specific antibodies were added before the formation of DNA-protein complexes at 25 °C for 15 min.

Immunoprecipitation and immunoblot analysis. Nuclear extracts, cytoplasmic extracts and total cell lysates from CD4⁺ T cells (2.5–10 μg) were separated by 10% SDS-PAGE and were blotted onto polyvinylidene difluoride membranes. Blotted membranes were incubated with antibodies specific for NF-κB subunits, followed by incubation with goat anti-mouse, or donkey anti-rabbit coupled to horseradish peroxidase, and proteins were made visible with the SuperSignal West Pico Chemiluminescent Substrate (Pierce). For immunoprecipitation, purified proteins (10–50 μg) 'captured' with the antibody were

incubated with immobilized protein G and were precipitated with a Seize Classic Mammalian Immunoprecipitation Kit (Pierce). Precipitated proteins were analyzed by immunoblot with the NF-κB subunit-specific antibodies described above and a Rabbit IgG TrueBlot set (eBioscience). Positive controls for the detection of NF-κB subunits were confirmed by immunoblot analysis (Supplementary Fig. 6 online) using Jurkat or A431 cell lysates (BD Transduction Laboratories).

ELISA. The amount of IL-2 and IL-10 proteins in culture supernatants was determined by ELISA. Production of transforming growth factor-β was measured with the DuoSet ELISA Development System (R&D Systems). For this, 96-well flat-bottomed plates were precoated with capture antibodies, and diluted samples or standard recombinant cytokines were added to each well. After plates were washed, biotinylated antibodies were added and then wells were incubated with horseradish peroxidase-labeled, affinity-purified anti-rat immunoglobulin G (IgG). A solution of *o*-phenyldiamine (Sigma) was added to each well as a substrate. The optical density at 490 nm was measured with a microplate reader (Molecular Devices).

Confocal microscopy. Cells were deposited onto poly-L-lysine-coated glass slides, were fixed with 3% paraformaldehyde in PBS, were made permeable for 2 min with 0.2% Triton X-100 in PBS and were preblocked for 1 h with 1% BSA and 2.5% FCS in PBS. Cells were stained for 1 h with 1 μg/ml of the appropriate primary antibodies. After being washed three times with 0.0001% Triton X-100 in PBS, cells were stained for 30 min with secondary Alexa Fluor 488-conjugated donkey anti-mouse or goat anti-rabbit IgG (heavy plus light) and then were washed with PBS. Coverslips were applied with Fluoromount-G (Molecular Probes). Cells were visualized with a BioRad 1024 laser-scanning confocal microscope (BioRad Laboratories). Each optical section was acquired sequentially with 488-nm and 568-nm laser lines to excite Alexa Fluor 488 (green) and Alexa Fluor 568 (red) fluorescence, respectively. Merged images are presented as yellow. For FRET, Zenon Rabbit IgG Labeling Kits or Zenon Mouse IgG Labeling Kits (Molecular Probe) were used to label antibodies with Alexa Fluor 488 as the 'donor dye' or Alexa Fluor 546 as the 'acceptor dye'⁵³. Red color indicates that the acceptor dye was activated by the donor dye, as the two dyes were in close proximity.

NF-κB transcription activity assay. The transcriptional activity of NF-κB subunits of the nuclear extracts from naive T cells was analyzed with NF-κB Family Transcription Factor Assay Kit (Chemicon). Nuclear extracts were incubated with biotinylated double-stranded oligonucleotide probe containing the consensus sequence (5'-GGGACTTCC-3') for NF-κB on a streptavidin-coated plate. Captured complexes, including active NF-κB protein, were incubated with the primary antibody for NF-κB subunit and horseradish peroxidase-conjugated secondary antibody and tetramethylbenzidine substrate. The absorbance of the samples was measured with a spectrophotometry microplate reader set at 450 nm.

Pulse-chase assay. Purified naive CD4⁺ T cells from *aly/+* and *aly/aly* mice were cultured for 4 h in methionine-free RPMI 1640 medium (Sigma) supplemented with ³⁵S-labeled methionine (50 μCi/ml) on plates coated with mAbs to TCR and CD28. Purified total extracts were immunoprecipitated with rabbit anti-RelA. Radiolabeled proteins in the immunoprecipitate were resolved by reduced SDS-PAGE; the dried gel was exposed to autoradiography film in a phosphorimaging cassette.

Cell transfer. CFSE-labeled naive or memory CD4⁺ T cells (5 × 10⁶) from *aly/aly*, *aly/+* or B6.Ly5.1 mice were transferred intravenously into irradiated (700 cGy) B6.PL (Thy-1.1⁺) or B6 mice. On day 7 after transfer, spleen cells were analyzed to measure homeostatic proliferation via CFSE dilution by flow cytometry. For analysis of *in vivo* antigen-specific T cell responses, 5 × 10⁶ CFSE-labeled naive CD4⁺ T cells from *aly/aly* OT-II B6.PL and *aly/+* OT-II B6.PL mice were transferred intravenously into B6 mice; OVA peptide of amino acids 323–339 (0–200 μg) was injected intraperitoneally into the mice; 3 d later, proliferation of the donor cells in spleen and lymph node was analyzed by flow cytometry. For induction of autoimmune lesions in *aly/aly* mice, 5 × 10⁶ enriched total CD4⁺, CD25⁺CD4⁺ or naive CD4⁺ cells from *aly/+* or *aly/aly* mice were transferred intravenously into *Rag2^{-/-}* mice.

Histological analysis. All organs of *Rag2*^{-/-} mice that had received cell transfer were removed, were fixed with 4% phosphate-buffered formaldehyde, pH 7.2, and were prepared for histological examination. Sections were stained with hematoxylin and eosin. The disease incidence and severity in pancreata and lacrimal glands was determined by the histological score of inflammatory lesions as described⁵⁴. For the inflammatory lesions of lungs, lymphocytes per mm² were counted. Histological findings were estimated by three independent, well-trained pathologists 'blinded' to sample identity.

Statistics. Student's *t*-test was used for statistical analyses.

Note: Supplementary information is available on the Nature Immunology website.

ACKNOWLEDGMENTS

We thank B. Marchand for typing the manuscript. Supported by the United States Public Health Service (CA38355, AI21487, AI46710 and AG01743; publication number 17327-IMM from The Scripps Research Institute) and by the Ministry of Education, Science, and Culture of Japan (grants-in-aid for scientific research; 17689049).

COMPETING INTERESTS STATEMENT

The authors declare that they have no competing financial interests.

Published online at <http://www.nature.com/natureimmunology/>

Reprints and permissions information is available online at <http://npg.nature.com/reprintsandpermissions/>

- Ghosh, S., May, M.J. & Kopp, E.B. NF- κ B and Rel proteins: evolutionarily conserved mediators of immune responses. *Annu. Rev. Immunol.* **16**, 225–260 (1998).
- Karin, M. How NF- κ B is activated: the role of the I κ B kinase (IKK) complex. *Oncogene* **18**, 6867–6874 (1999).
- Bonizzi, G. & Karin, M. The two NF- κ B activation pathways and their role in innate and adaptive immunity. *Trends Immunol.* **25**, 280–288 (2004).
- Kahn-Perles, B., Lipcey, C., Lecine, P., Olive, D. & Imbert, J. Temporal and subunit-specific modulations of the Rel/NF- κ B transcription factors through CD28 costimulation. *J. Biol. Chem.* **272**, 21774–21783 (1997).
- Sun, Z. *et al.* PKC- θ is required for TCR-induced NF- κ B activation in mature but not immature T lymphocytes. *Nature* **404**, 402–407 (2000).
- Ruland, J. *et al.* Bcl10 is a positive regulator of antigen receptor-induced activation of NF- κ B and neural tube closure. *Cell* **104**, 33–42 (2001).
- Thome, M. & Tschopp, J. TCR-induced NF- κ B activation: a crucial role for Carma1, Bcl10 and MALT1. *Trends Immunol.* **24**, 419–424 (2003).
- Karin, M. & Ben-Neriah, Y. Phosphorylation meets ubiquitination: the control of NF- κ B activity. *Annu. Rev. Immunol.* **18**, 621–663 (2000).
- Pimentel-Muinos, F. *et al.* Regulation of interleukin-2 α chain expression and nuclear factor κ B activation by protein kinase C in T lymphocytes. Autocrine role of tumor necrosis factor α . *J. Biol. Chem.* **269**, 24424–24429 (1994).
- Prasad, A.S. *et al.* Zinc enhances the expression of interleukin-2 and interleukin-2 receptors in HUF-78 cells by way of NF- κ B activation. *J. Lab. Clin. Med.* **140**, 272–289 (2002).
- Dejardin, E. *et al.* The lymphotoxin- β receptor induces different patterns of gene expression via two NF- κ B pathways. *Immunity* **17**, 525–535 (2002).
- Matsushima, A. *et al.* Essential role of nuclear factor (NF)- κ B-inducing kinase and inhibitor of κ B (I κ B) kinase α in NF- κ B activation through lymphotoxin β receptor, but not through tumor necrosis factor receptor 1. *J. Exp. Med.* **193**, 631–636 (2001).
- Matsumoto, M. *et al.* Essential role of NF- κ B-inducing kinase in T cell activation through the TCR/CD3 pathway. *J. Immunol.* **169**, 1151–1158 (2002).
- Artis, D. *et al.* NF- κ B1 is required for optimal CD4⁺ Th1 cell development and resistance to *Leishmania major*. *J. Immunol.* **170**, 1995–2003 (2003).
- Erdman, S., Fox, J.G., Dangler, C.A., Feldman, D. & Horwitz, B.H. Typhlocolitis in NF- κ B-deficient mice. *J. Immunol.* **166**, 1443–1447 (2001).
- Hilliard, B., Samoilova, E.B., Liu, T.S., Rostami, A. & Chen, Y. Experimental autoimmune encephalomyelitis in NF- κ B-deficient mice: roles of NF- κ B in the activation and differentiation of autoreactive T cells. *J. Immunol.* **163**, 2937–2943 (1999).
- Das, J. *et al.* A critical role for NF- κ B in GATA3 expression and Th₂ differentiation in allergic airway inflammation. *Nat. Immunol.* **2**, 45–50 (2001).
- Beg, A.A., Sha, W.C., Bronson, R.T., Ghosh, S. & Baltimore, D. Embryonic lethality and liver degeneration in mice lacking the RelA component of NF- κ B. *Nature* **376**, 167–170 (1995).
- Burkly, L. *et al.* Expression of RelB is required for the development of thymic medulla and dendritic cells. *Nature* **373**, 531–536 (1995).
- Wei, F. *et al.* Multiorgan inflammation and hematopoietic abnormalities in mice with a targeted disruption of RelB, a member of the NF- κ B/Rel family. *Cell* **80**, 331–340 (1995).
- Franzoso, G. *et al.* Mice deficient in nuclear factor (NF)- κ B/p52 present with defects in humoral responses, germinal center reactions, and splenic microarchitecture. *J. Exp. Med.* **187**, 147–159 (1998).
- Speirs, K., Lieberman, L., Caamano, J., Hunter, C.A. & Scott, P. Cutting edge: NF- κ B2 is a negative regulator of dendritic cell function. *J. Immunol.* **172**, 752–756 (2004).
- Hilliard, B.A. *et al.* Critical roles of c-Rel in autoimmune inflammation and helper T cell differentiation. *J. Clin. Invest.* **110**, 843–850 (2002).
- Kontgen, F. *et al.* Mice lacking the c-rel proto-oncogene exhibit defects in lymphocyte proliferation, humoral immunity, and interleukin-2 expression. *Genes Dev.* **9**, 1965–1977 (1995).
- Shinkura, R. *et al.* Alymphoplasia is caused by a point mutation in the mouse gene encoding NF- κ B-inducing kinase. *Nat. Genet.* **22**, 74–77 (1999).
- Novack, D.V. *et al.* The I κ B function of NF- κ B2 p100 controls stimulated osteoclastogenesis. *J. Exp. Med.* **198**, 771–781 (2003).
- Yin, L. *et al.* Defective lymphotoxin- β receptor-induced NF- κ B transcriptional activity in NIK-deficient mice. *Science* **291**, 2162–2165 (2001).
- Fagarasan, S. *et al.* Alymphoplasia (aly)-type nuclear factor κ B-inducing kinase (NIK) causes defects in secondary lymphoid tissue chemokine receptor signaling and homing of peritoneal cells to the gut-associated lymphatic tissue system. *J. Exp. Med.* **191**, 1477–1486 (2000).
- Yamada, T. *et al.* Abnormal immune function of hemopoietic cells from alymphoplasia (aly) mice, a natural strain with mutant NF- κ B-inducing kinase. *J. Immunol.* **165**, 804–812 (2000).
- Kajitara, F. *et al.* NF- κ B-inducing kinase establishes self-tolerance in a thymic stroma-dependent manner. *J. Immunol.* **172**, 2067–2075 (2004).
- Wei, F. *et al.* Both multiorgan inflammation and myeloid hyperplasia in RelB-deficient mice are T cell dependent. *J. Immunol.* **157**, 3974–3979 (1996).
- Tsubata, R. *et al.* Autoimmune disease of exocrine organs in immunodeficient alymphoplasia mice: a spontaneous model for Sjogren's syndrome. *Eur. J. Immunol.* **26**, 2742–2748 (1996).
- Dutton, R.W., Bradley, L.M. & Swain, S.L. T cell memory. *Annu. Rev. Immunol.* **16**, 201–223 (1998).
- Sprent, J. & Surh, C.D. T cell memory. *Annu. Rev. Immunol.* **20**, 551–579 (2002).
- Sakaguchi, S. Naturally arising CD4⁺ regulatory T cells for immunologic self-tolerance and negative control of immune responses. *Annu. Rev. Immunol.* **22**, 531–562 (2004).
- Fehervari, Z. & Sakaguchi, S. Development and function of CD25⁺CD4⁺ regulatory T cells. *Curr. Opin. Immunol.* **16**, 203–208 (2004).
- Piccirillo, C.A. & Shevach, E.M. Naturally-occurring CD4⁺CD25⁺ immunoregulatory T cells: central players in the arena of peripheral tolerance. *Semin. Immunol.* **16**, 81–88 (2004).
- Khattri, R., Cox, T., Yasayko, S.A. & Ramsdell, F. An essential role for Scurfin in CD4⁺CD25⁺ T regulatory cells. *Nat. Immunol.* **4**, 337–342 (2003).
- Fontenot, J.D., Gavin, M.A. & Rudensky, A.Y. Foxp3 programs the development and function of CD4⁺CD25⁺ regulatory T cells. *Nat. Immunol.* **4**, 330–336 (2003).
- Hori, S., Nomura, T. & Sakaguchi, S. Control of regulatory T cell development by the transcription factor Foxp3. *Science* **299**, 1057–1061 (2003).
- Lu, L.F., Gondek, D.C., Scott, Z.A. & Noelle, R.J. NF κ B-inducing kinase deficiency results in the development of a subset of regulatory T cells, which shows a hyperproliferative activity upon glucocorticoid-induced TNF receptor family-related gene stimulation. *J. Immunol.* **175**, 1651–1657 (2005).
- Ernst, B., Lee, D.-S., Chang, J., Sprent, J. & Surh, C.D. The peptide ligands mediating positive selection in the thymus control T cell survival and homeostatic proliferation in the periphery. *Immunity* **11**, 173–181 (1999).
- Weil, R. & Israel, A. T-cell-receptor- and B-cell-receptor-mediated activation of NF- κ B in lymphocytes. *Curr. Opin. Immunol.* **16**, 374–381 (2004).
- Kim, H.P. & Leonard, W.J. The basis for TCR-mediated regulation of the IL-2 receptor α chain gene: role of widely separated regulatory elements. *EMBO J.* **21**, 3051–3059 (2002).
- Schuh, K. *et al.* The interleukin 2 receptor α chain/CD25 promoter is a target for nuclear factor of activated T cells. *J. Exp. Med.* **188**, 1369–1373 (1998).
- Bren, G.D. *et al.* Transcription of the RelB gene is regulated by NF- κ B. *Oncogene* **20**, 7722–7733 (2001).
- Olahaw, N.E. Inducible activation of RelB in fibroblasts. *J. Biol. Chem.* **271**, 30307–30310 (1996).
- Ivanov, V.N., Deng, G., Podack, E.R. & Malek, T.R. Pleiotropic effects of Bcl-2 on transcription factors in T cells: potential role of NF- κ B p50-p50 for the anti-apoptotic function of Bcl-2. *Int. Immunol.* **7**, 1709–1720 (1995).
- Robertson, J.M., Jensen, P.E. & Evavold, B.D. DO11.10 and OT-II T cells recognize a C-terminal ovalbumin 323–339 epitope. *J. Immunol.* **164**, 4706–4712 (2000).
- Kishimoto, H. & Sprent, J. Strong TCR ligation without costimulation causes rapid onset of Fas-dependent apoptosis of naive murine CD4⁺ T cells. *J. Immunol.* **163**, 1817–1826 (1999).
- Assenmacher, M., Schmitz, J. & Radbruch, A. Flow cytometric determination of cytokines in activated murine T helper lymphocytes: expression of interleukin-10 in interferon- γ and interleukin-4-expressing cells. *Eur. J. Immunol.* **24**, 1097–1101 (1994).
- Grundstrom, S., Anderson, P., Scheipers, P. & Sundstedt, A. Bcl-3 and NF κ B p50-p50 homodimers act as transcriptional repressors in tolerant CD4⁺ T cells. *J. Biol. Chem.* **279**, 8460–8468 (2004).
- Zal, T. & Gascoigne, N.R. Using live FRET imaging to reveal early protein-protein interactions during T cell activation. *Curr. Opin. Immunol.* **16**, 418–427 (2004).
- Ishimaru, N. *et al.* Development of autoimmune exocrinopathy resembling Sjogren's syndrome in estrogen-deficient mice of healthy background. *Am. J. Pathol.* **163**, 1481–1490 (2003).

Novel Role for RbAp48 in Tissue-Specific, Estrogen Deficiency-Dependent Apoptosis in the Exocrine Glands

Naozumi Ishimaru,¹ Rieko Arakaki,¹ Fumie Omotehara,¹ Koichi Yamada,² Kenji Mishima,² Ichiro Saito,² and Yoshio Hayashi^{1*}

Department of Oral Molecular Pathology, Institute of Health Biosciences, The University of Tokushima Graduate School, 3 Kuramotocho, Tokushima 770-8504,¹ and Department of Pathology, Tsurumi University School of Dentistry, Tsurumi,² Japan

Received 1 August 2005/Returned for modification 31 August 2005/Accepted 20 January 2006

Although tissue-specific apoptosis in the exocrine glands in estrogen-deficient mice may contribute to the development of autoimmune exocrinopathy, the molecular mechanism responsible for tissue-specific apoptosis remains obscure. Here we show that RbAp48 overexpression induces p53-mediated apoptosis in the exocrine glands caused by estrogen deficiency. RbAp48-inducible transfectant results in rapid apoptosis with p53 phosphorylation (Ser9) and α -fodrin cleavage. Reducing the expression of RbAp48 through small interfering RNA inhibits the apoptosis. Prominent RbAp48 expression with apoptosis was observed in the exocrine glands of C57BL/6 ovariectomized (OVX) mice but not in OVX estrogen receptor $\alpha^{-/-}$, p53 $^{-/-}$, and E2F-1 $^{-/-}$ mice. Indeed, transgenic expression of the RbAp48 gene induced apoptosis in the exocrine glands but not in other organs. These findings indicate that estrogen deficiency initiates p53-mediated apoptosis in the exocrine gland cells through RbAp48 overexpression and exerts a possible gender-based risk of autoimmune exocrinopathy in postmenopausal women.

Estrogenic action has been suggested to be responsible for the strong female preponderance of many autoimmune diseases, including systemic lupus erythematosus, rheumatoid arthritis, and Sjögren's syndrome (50, 51). Recent evidence suggests that apoptosis plays a key role in the physiology and pathogenesis of various autoimmune diseases (2, 7, 19, 35, 42). We have demonstrated that estrogenic action influences target epithelial cells through Fas-mediated apoptosis in a murine model for Sjögren's syndrome (13). Recently, we found that tissue-specific apoptosis in the exocrine glands spontaneously occurring in estrogen-deficient mice may contribute to the development of autoimmune exocrinopathy (14). We speculate that antiestrogenic actions might be a potent factor in the formation of pathogenic autoantigens. It has been reported that the antiestrogen tamoxifen (TAM) induces cell death in the human breast cancer cell line MCF-7 (17). We observed a time- and concentration-dependent increase in apoptosis of mouse and human salivary gland cells ([MSG] mouse primary culture; [HSG] human cell line) treated with TAM but not in other cell lines (HT-29, Colo201, and Jurkat) (14).

Apoptosis can be initiated by many different factors, but activation of caspases, which are a special class of proteolytic enzymes, is always involved in this process. Activation of caspases may be achieved by several molecular pathways; the best known stimuli triggering the caspase cascade are stimulation of Fas or TNF receptors, release of cytochrome *c* from the cellular mitochondria, and exposure to granzymes, which are secreted by cytotoxic T cells (3, 12, 31, 37, 54). Detailed research on the mechanisms controlling caspase activity will pro-

vide better insight into the pathogenesis of autoimmune diseases with special reference to estrogen deficiency. In this study, we have focused on the molecular mechanisms responsible for tissue-specific apoptosis caused by estrogen deficiency and identified RbAp48 as a novel apoptosis-inducing gene exclusively in the exocrine glands. Retinoblastoma (Rb) protein is a multifunctional protein that binds to transcription factors and kinases to regulate both cell growth and apoptosis (11). Although recent data suggest that loss of Rb can cause apoptosis through derepression of basally inhibited extrinsic apoptotic pathway genes (20), no mechanism has provided a molecular explanation for RbAp48 in the induction of apoptosis.

MATERIALS AND METHODS

Cell culture and gene transfection. HSG, MSG, HT29, Colo201, HeLa, HepG2, SH-SY5Y, NEC14, THP-1, Jurkat, Raji, U937, and W138 cells were cultured in Dulbecco's modified Eagle medium (DMEM) or RPMI 1640 medium containing 10% fetal bovine serum at 37°C. HSG and MSG cells have been described elsewhere (38, 40). The following were used for cell cultures: 10⁻⁷ M TAM (Wako Pure Chemical, Osaka, Japan), 10⁻⁹ M β -2-estradiol (E2; Wako), 10⁻⁷ M staurosporin (Wako), paclitaxel (Wako), 1 μ M etoposide (Wako), 1 μ M ICI182780 (Wako), 25 ng/ml anti-Fas monoclonal antibody (MAb) (MBL, Nagoya, Japan), and 10 ng/ml recombinant human gamma interferon (R&D Systems, Minneapolis, MN). The RbAp48 gene inserted into the pCMV (2N3T) vector, a gift from D. Trouche, was transfected into the cells using FuGENE6 Transfection Reagent (Roche Diagnostics Corp., Indianapolis, IN). The RbAp48-stable cell line (RH0) from HSG cells in which RbAp48 expression was regulated by isopropyl-1-thio- β -D-galactopyranoside (IPTG), was established using a LacSwitch II Inducible Mammalian Expression System (Stratagene, La Jolla, CA). Briefly, the repressor vector (pCMVlacI) and RbAp48-inserted operator vector (pOPRV1/MCS) were cotransfected into HSG cells with FuGENE6, and the RbAp48 expression of hygromycin and G418-resistant transfectants was controlled by IPTG. For infection of adenovirus vector, RbAp48 gene-transfected MSG cells from p53 $^{-/-}$ or wild-type mice were infected with 100 multiplicities of infection of adenovirus vector including the p53 gene obtained from Toren Finkel (National Institutes of Health). MSG and mouse mammary glands (MMG) were removed, placed in DMEM containing 10% fetal calf serum (FCS) and 10 mM HEPES (pH 7.4), and rapidly minced. The mate-

* Corresponding author. Mailing address: Department of Oral Molecular Pathology, Institute of Health Biosciences, The University of Tokushima Graduate School, 3 Kuramotocho, Tokushima 770-8504, Japan. Phone: 81 88 633 7327. Fax: 81 88 633 7327. E-mail: hayashi@dent.tokushima-u.ac.jp.

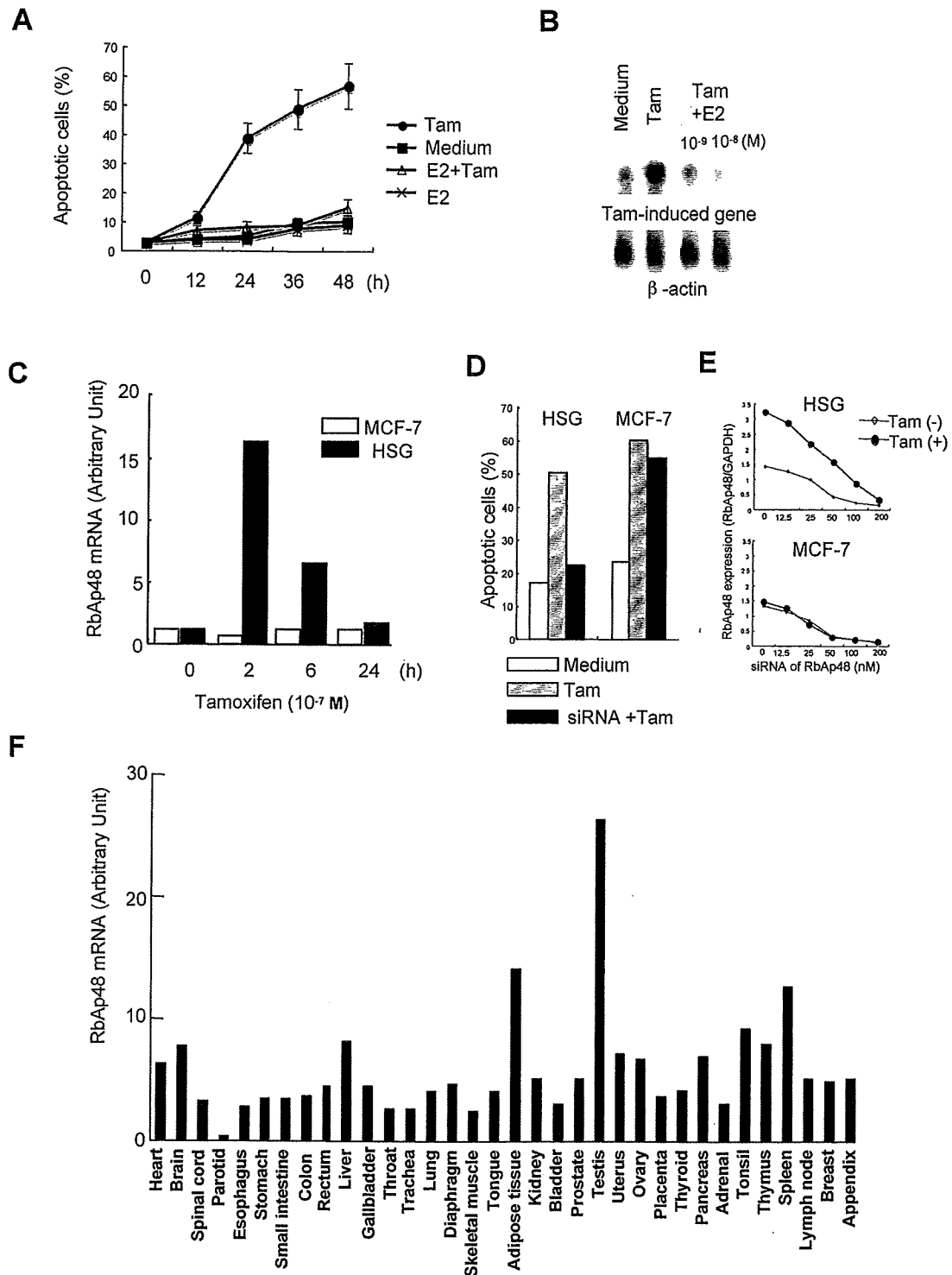


FIG. 1. Identification of the RbAp48 gene in salivary gland cell apoptosis. (A) A time-dependent increase in apoptotic HSG cells stimulated with TAM (10^{-7} M) was observed, and E2 (10^{-9} M) treatment inhibited apoptosis. Apoptotic cells were detected by flow cytometry using FITC-conjugated annexin V. (B) TAM-induced gene fragments cloned by differential display PCR were used as a probe by Northern blotting with mRNA from HSG cells treated with TAM (10^{-7} M) or E2 (10^{-9} M and 10^{-8} M). β -Actin mRNA was detected as an internal control. Each blot is representative of three independent experiments. (C) Analysis of RbAp48 mRNA expression was performed using total RNA from TAM-stimulated HSG and MCF-7 cells for 0 to 24 h. The graph is representative of three independent experiments. (D) The inhibitory effects of siRNA on TAM-induced apoptosis in HSG cells with siRNA (15 nM) of the RbAp48 construct but not in MCF-7 cells. After transfection of siRNA of RbAp48 and a fluorescence-labeled control gene, the cells were incubated with TAM (10^{-7} M) for an additional 24 h. Apoptosis was estimated by flow cytometric analysis using PE-conjugated annexin V. The graph is representative of three independent experiments. (E) A dose-dependent inhibition of siRNA (0 to 200 nM) of TAM-induced RbAp48 expression in HSG cells, not MCF-7 cells, was observed. The graph is representative of two independent experiments. (F) RbAp48 mRNA expression levels were analyzed using human tissue total RNA-blotted membrane. Message levels (arbitrary units) were quantified by BAS-2000II and expressed as the ratio of RbAp48 mRNA/ β -actin mRNA. The graph is representative of two independent experiments.

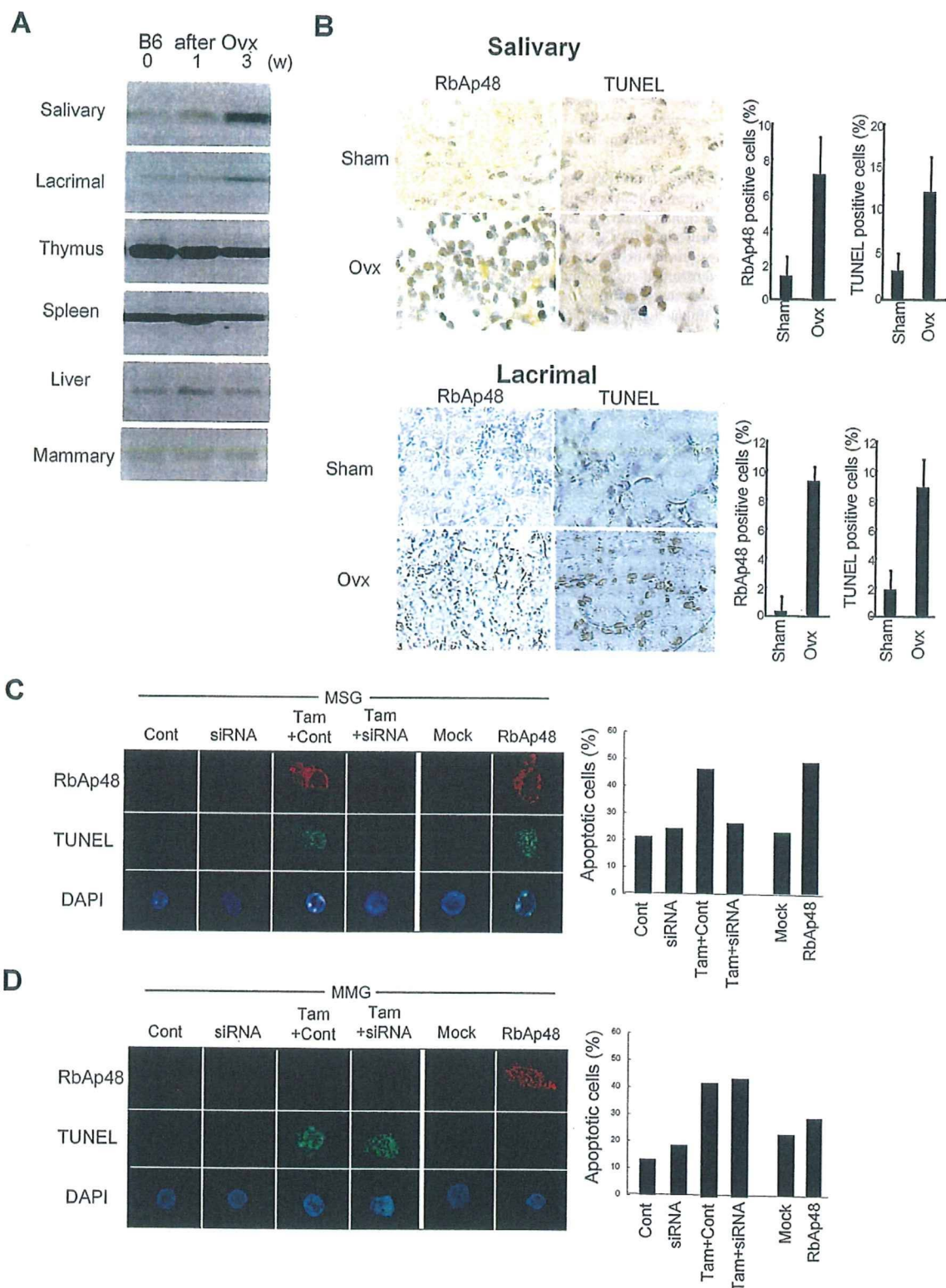


FIG. 2. RbAp48 overexpression in OVX B6 mice. (A) Increased RbAp48 expression in salivary and lacrimal gland tissues in OVX B6 mice from 0 to 3 weeks (age of mice, 4 to 7 weeks). Expression levels of RbAp48 in thymus, spleen, liver, and mammary glands from OVX B6 mice were constant. Western blot analysis was performed on proteins from tissue homogenates of OVX and sham mice. Blots were representative of three independent experiments. (B) Detection of RbAp48⁺ and TUNEL⁺ cells in salivary and lacrimal glands from OVX B6 and sham B6 mice at the age of 7 weeks. Immunohistochemical analysis of RbAp48 and in situ TUNEL assays were performed on the sections of salivary and lacrimal glands from OVX and sham mice. Images are representative of sections from five mice. The percentage of RbAp48⁺ and TUNEL⁺ cells in salivary and lacrimal glands was enumerated using a 10- by 20-mm grid covering an objective area of 0.16 mm². Data were analyzed in 10 fields per section and expressed as mean percent \pm standard deviation of data from five mice. (C) TAM-induced apoptosis was associated with RbAp48 expression in

rials were then digested for 1 h at 37°C with 750 U/ml collagenase (Wako), 500 U/ml hyaluronidase type IV (Sigma), 1% bovine serum albumin, and 10 mM HEPES (pH 7.4) in DMEM. After digestion, they were filtered through a 70- μ m nylon mesh, centrifuged, and rinsed twice with DMEM containing 10% FCS. These cells were cultured in chamber slides (Nalge Nunc International, Denmark) at a density of 5×10^4 /well with DMEM containing 10% FCS. After cells were cultured for 24 h, the medium was changed to HuMedia-KG2 (Kurabo, Osaka, Japan).

Differential display analysis and Northern blotting. Total RNA was isolated from TAM-treated or nontreated HSG cells and reverse transcribed for differential display PCR with an RNAmage kit (Gene Hunter, Nashville, TN). TAM-induced cDNA fragments were gel excised and subcloned for TA vector. The clones were screened with a cDNA library derived from mRNA of TAM-stimulated HSG cells. The screened clone was transformed to plasmid and sequenced. Expressions of RbAp48 mRNA were detected by Northern blot analysis using 32 P-labeled RbAp48 cDNA probe. Equal loading of the gel was confirmed by using β -actin cDNA probe. In addition, the human total RNA-blotted membrane (Biocoin Institute, Inc., San Leandro, CA) was used for analysis of RbAp48 mRNA in various human tissues.

Apoptosis detection assay. Apoptosis was detected using the annexin V-fluorescein isothiocyanate (FITC) apoptosis detection kit (Genzyme Corp., Cambridge, MA). Briefly, after cultured cells were washed with phosphate-buffered saline, the cells were incubated with FITC-conjugated annexin V and propidium iodide (PI) for 10 min at room temperature in the dark. Binding buffer was added, and apoptotic cells were detected by flow cytometric analysis with an EPICS flow cytometer (Beckman Coulter, Inc., Miami, FL).

Mice. Estrogen receptor α -deficient (ER $\alpha^{-/-}$), p53 $^{-/-}$, E2F-1 $^{-/-}$, or C57BL/6 (B6) mice were purchased from Taconic (Germantown, NY), Jackson Laboratory (Bar Harbor, ME), or Nihon Clea (Tokyo, Japan). These mice were subjected to ovariectomy (OVX mice) and or to a sham operation (sham mice) at 4 weeks of age. At 0 to 3 weeks after OVX, all organs were evaluated by pathological or immunohistochemical analysis. To generate the RbAp48-transgenic (TG) mice, B6 mice were used to obtain fertilized eggs, and the gene fragment containing RbAp48 cDNA regulated by salivary gland-specific promoter (22) (provided by B. B. Larsen) was microinjected into the pronucleus of fertilized eggs to establish the transgenic lines. Histopathological analysis of all organs of RbAp48-TG mice screened by PCR was performed. All mice were maintained in our specific-pathogen-free facility.

siRNA of RbAp48. Small interfering RNA (siRNA) corresponding to the coding sequence +136 to +156 of the RbAp48 gene was synthesized by Hokkaido System Science (Sapporo, Japan) according to standard methods (23, 52) for the following: sense, CGAGGAAUACAAAUAUGGTT; antisense, CCAUAAUUUGUAUCCUCGTT. siRNA of the glyceraldehyde-3-phosphate dehydrogenase (GAPDH) gene (Ambion, Austin, TX) was used as a control. siRNA (0 to 50 nM) and 1 μ g of pCMV-green fluorescent protein (GFP) plasmid were cotransfected into HSG, MCF-7 cells, and the IPTG-controlled RbAp48-stable cell line (RH0) using a Silencer siRNA Transfection II Kit (Ambion) or FuGENE6 (Roche). At 24 h after cotransfection, RH0 cells were incubated with IPTG for an additional 24 h. GFP $^{+}$ apoptotic cells were detected by flow cytometry using phycoerythrin (PE)-conjugated annexin V.

E2F-1, ARF, and p53 siRNA. For siRNA of E2F-1, ARF, and p53, a siTrio Full Set (B-Brigide International, Sunnyvale, CA) was used for HSG cells. Briefly, each cocktail including the three RNA oligonucleotides listed below was transfected into cells with a Quick-Step Transfection Kit (B-Brigide International). Sequences of the oligonucleotide sets are as follows: for E2F-1, CCAACGUCCUUGAGGGCAUITT (sense), AUGCCUCAAGGACGUUGGTT (antisense), CUGCAGAGCAGAUGGUUAUITT (sense), AUAACCAUCUGCUCGAGTT (antisense), GGAAGUGAGGGAGGGAGATT (sense), and UCUCUCCUCCUCACUUUCCTT (antisense); for ARF, GCUCACUCUGGUCGCAAITT (sense), UACCAAGAACCUGCGCACTT (antisense), GGGUUUUUCGCGGUUCACAUUITT (sense), AUGUGAACCACGAAAACCTT (antisense), GGGUUUUUCGUGGUUCACAUUITT (sense), and AUGUGAACCACGAAAACCTT (antisense), UUUUCAGGAAGUAGUUUCCTT (antisense), CUGGAAGACUCCAGUGGUUUITT (sense), UACCACUGGAGUCUUCAGTT (antisense), CUUAGUACCUAAA

AGGAAATT (sense), and UUUCCUUUUAGGUACUAAGTT (antisense). Transfected cells were incubated with or without TAM, and confocal or flow cytometric analysis was performed.

Western blotting. Whole-cell extracts of HSG or RH0 cells were purified using radioimmunoprecipitation assay buffer (50 mM Tris-HCl, pH 7.4, 150 mM NaCl, 1 mM EDTA, 1% NP-40, 1 mM dithiothreitol [DTT], 1 mM phenylmethylsulfonyl fluoride) supplemented with a protease inhibitor cocktail (Sigma Chemical Co., St. Louis, MO). After centrifugation for 20 min at 12,000 rpm at 4°C, the supernatant was extracted and used for samples. Also, to detect α -fodrin in organs, tissue samples from OVX and sham C57BL/6 mice were extracted as described above. Ten micrograms of each sample per well was used for 7.5 to 12.5% sodium dodecyl sulfate-polyacrylamide gel electrophoresis and transferred to polyvinylidene difluoride membranes, which were probed with anti-RbAp48, anti-Rb (p110 and p130), anti-Bad, anti-Bax, anti-ARF (p14 and p19), anti-cyclin D3 (BD Transduction Laboratories, Lexington, KY), anti-Mdm2, anti-E2F-1, anti-phospho-Rb (Sigma), anti-p53, anti-phospho-p53 Ab sampler kit (Ser6, Ser9, Ser15, Ser20, Ser37, Ser46, and Ser392; Cell Signaling Technology Inc., Beverly, MA), anti- α -fodrin (Affinity, Mamhead, United Kingdom), and anti-p21 (Santa Cruz Biotechnology, Santa Cruz, CA) as the primary Abs, and anti- α -tubulin, GAPDH, or histone MAb (Sigma) as internal control. The nitrocellulose membranes were incubated with peroxidase-conjugated horse anti-mouse or rabbit immunoglobulin G (IgG; Vector Laboratories) as the secondary Ab. Protein binding was visualized with ECL Western blotting reagent (Amersham Corp., Arlington Heights, IL).

TUNEL assay. Apoptotic cells were detected in sections using the in situ terminal deoxynucleotidyltransferase (TdT)-mediated dUTP-biotin nick end labeling (TUNEL) kit (Wako). Sections were incubated with proteinase K (20 μ g/ml) for 10 min and then presoaked in TdT buffer (0.5 μ M cacodylate, 1 mM CoCl $_2$, 0.5 μ M DTT, 0.05% bovine serum albumin, 0.15 M NaCl) for 10 min. Sections were incubated for 2 h at 37°C in 25 μ l of TdT solution, containing 1 \times terminal transferase buffer, 0.5 nmol of biotin-dUTP, and 10 U of TdT. After the TdT reaction, sections were soaked in TdT blocking buffer (300 nM NaCl, 30 mM Tris-sodium citrate-2-hydrate), incubated with horseradish peroxidase-conjugated streptavidin for 30 min at room temperature, and developed for 10 min in phosphate-buffered citrate (pH 5.8) containing 0.6 mg/ml DAB (3,3'-diaminobenzidine-tetrahydrochloride-dihydrate). Nuclei were counterstained with hematoxylin. For confocal microscopic analysis, FITC-labeled UTP was used.

Caspase activity assay. Caspase activities were assayed using a caspase family colorimetric substrate set (BioVision Inc.). Briefly, 100 μ g of cytoplasmic lysates of RH0 cells was incubated with 200 μ M Ac-YVAD-pNA (caspase 1 substrate), Ac-YVDAD-pNA (caspase 2 substrate), Ac-DEVD-pNA (caspase 3 substrate), Ac-WEHD-pNA (caspase 5 substrate), Ac-VEID-pNA (caspase 6 substrate), Ac-IETD-pNA (caspase 8 substrate), and Ac-LEHD-pNA (caspase 9 substrate) at 37°C for 1 h. The absorbance of samples was read at 405 nm in a microtiter plate reader. The relative percent increase in caspase activity was determined by comparing these results with the level of the uninduced control.

Gel shift assay. Nuclear extracts were prepared from RH0 cells by a method previously described (29). Nuclear extracts containing 5 μ g of protein were incubated in 20 μ l of binding buffer (10 mM Tris-HCl, pH 8.0, 50 mM NaCl, 1 mM MgCl $_2$, 0.5 mM DTT, and 4% glycerol) with or without a cold competitor. The E2F-1 DNA probe, 5'-TCCGTAGTTTTCCGCGCTTAAATTTGAGAAAGGGCGGAAACTAGTC-3' (10,000 cpm) labeled with [γ - 32 P]ATP was added, and the samples were incubated at room temperature for 20 min. Reaction mixtures were separated in a 4% polyacrylamide gel and autoradiographed on X-ray film (Fujifilm, Kanagawa, Japan).

Immunohistochemical analysis. Immunohistochemical analysis of RbAp48 expression was performed on the sections of salivary and lacrimal glands from sham, OVX B6, RbAp48-WT (wild type), and RbAp48-TG mice. Paraffin-embedded sections were stained with anti-RbAp48 MAb (BD Transduction Laboratories) as the primary Ab. Protein binding was detected with an LSAB2 kit containing horseradish peroxidase (DAKO, Carpinteria, CA) and DAB as a substrate. The counterstaining of nuclei was performed with hematoxylin.

Confocal microscopy. Confocal microscopic analysis of RbAp48, E2F-1, ARF, and p53 expression, and TUNEL-positive cells was performed on the cultured cells, and frozen sections of salivary glands from sham, OVX ER $\alpha^{-/-}$, p53 $^{-/-}$,

MSG cells from B6 mice, and the inhibitory effects with siRNA of RbAp48 construct were observed by confocal microscopic analysis. The percentage of TUNEL $^{+}$ apoptotic cells was enumerated as described. Cont, irrelevant siRNA control. Images are representative of three independent experiments. (D) TAM-induced apoptosis was not associated with RbAp48 expression in the primary culture of MMG cells from B6 mice. TUNEL $^{+}$ apoptotic cells were enumerated as described. Images are representative of three independent experiments.